

Lawrence Berkeley National Laboratory

LBL Publications

Title

Diversifying Isoprenoid Platforms via Atypical Carbon Substrates and Non-model Microorganisms

Permalink

<https://escholarship.org/uc/item/1dv3b95b>

Journal

Frontiers in Microbiology, 12

ISSN

1664-302X

Authors

Carruthers, David N

Lee, Taek Soon

Publication Date

2021

DOI

10.3389/fmicb.2021.791089

Peer reviewed

1 **Diversifying isoprenoid platforms via atypical carbon substrates and non-model microorganisms**

2
3 David N. Carruthers^{1,2}, Taek Soon Lee^{1,2,*}

4
5 ¹Joint BioEnergy Institute, 5885 Hollis Street, Emeryville, CA 94608, USA

6 ²Biological Systems and Engineering Division, Lawrence Berkeley National Laboratory, Berkeley, CA
7 94720, USA

8
9 *Correspondence

10 Taek Soon Lee, Joint BioEnergy Institute, 5885 Hollis Street, Emeryville, CA 94608, USA

11 tslee@lbl.gov

12
13 **Keywords:** isoprenoids, metabolic engineering, synthetic biology, non-model organisms, C1 metabolism,
14 terpenes

15
16 **Abstract:**

17
18 Isoprenoid compounds are biologically ubiquitous, and their characteristic modularity has afforded products
19 ranging from pharmaceuticals to biofuels. Isoprenoid production has been largely successful in *Escherichia*
20 *coli* and *Saccharomyces cerevisiae* with metabolic engineering of the mevalonate (MVA) and
21 methylerythritol phosphate (MEP) pathways coupled with the expression of heterologous terpene
22 synthases. Yet conventional microbial chassis pose several major obstacles to successful
23 commercialization including the affordability of sugar substrates at scale, precursor flux limitations, and
24 intermediate feedback-inhibition. Now, recent studies have challenged typical isoprenoid paradigms by
25 expanding the boundaries of terpene biosynthesis and using non-model organisms including those capable
26 of metabolizing atypical C1 substrates. Conversely, investigations of non-model organisms have historically
27 informed optimization in conventional microbes by tuning heterologous gene expression. Here, we review
28 advances in isoprenoid biosynthesis with specific focus on the synergy between model and non-model
29 organisms that may elevate the commercial viability of isoprenoid platforms by addressing the dichotomy
30 between high titer production and inexpensive substrates.

31 Introduction

32
33 Isoprenoids are ubiquitous across all domains of life and span a wide and varied range of natural products.
34 Isoprenoids are characterized by condensation of the five carbon precursor molecules isopentenyl
35 diphosphate (IPP) and dimethylallyl diphosphate (DMAPP), which are typically generated through either
36 the mevalonate (MVA) or methylerythritol phosphate (MEP) pathways. The ease with which specialized
37 synthases and cytochromes can conjugate or decorate these precursors has led to a uniquely diverse class
38 of chemicals. Estimates of natural isoprenoid compounds in the last several decades have steadily
39 increased from 20,000 (Chappell, 1995) to over 70,000 (Moser and Pichler, 2019). The advent of advanced
40 sequencing, -omics, and bioinformatics technologies coupled with protein structural software and flux
41 balance analyses have facilitated a veritable revolution in synthetic biology and assured the continued
42 elucidation of isoprenoid compounds through bioprospecting and biosynthetic efforts.
43

44 Isoprenoids serve a number of critical roles both as primary and secondary metabolites. Primary
45 metabolites are essential to cell survival and propagation. They include carotenoids that serve as auxiliary
46 molecules for photoprotection and antioxidants (carotene, lycopene, lutein, zeaxanthin) as well as sterols
47 that help maintain membrane structure. Other isoprenoids function as components of dolichols, quinones,
48 and essential proteins that aid in glycosylation and electron transport (Chappell, 1995). Secondary
49 isoprenoid metabolites impart a non-essential benefit to cells usually by providing some defensive benefit
50 or, in higher plants, hormone signaling. As for isoprenoids, these include pigments, fragrances, essential
51 oils, and defensive chemicals that are most prominent in higher plants. Many secondary metabolites have
52 attracted particular interest due to their applications as pharmaceuticals (e.g. artemisinin (Ro et al., 2006)
53 and paclitaxel (Biggs et al., 2016)), nutraceuticals, biofuels (e.g. isoprenol (Kang et al., 2019), prenol
54 (Zheng et al., 2013), bisabolene, and limonene (Alonso-Gutierrez et al., 2013)), and cosmetics (Schempp
55 et al., 2018). Hybrid technologies have capitalized on isoprenoid versatility through semi-synthetic
56 approaches to generate elastomers (Della Monica and Kleij, 2020). Collectively, the bioproduction of these
57 chemicals has enabled access to multibillion dollar chemical markets.
58

59 Microbial pathway engineering has proven especially successful in *Escherichia coli* and *Saccharomyces*
60 *cerevisiae*, which have produced many of the aforementioned isoprenoid compounds. *E. coli* and *S.*
61 *cerevisiae* maintain certain metabolic advantages including a fast growth phenotype, historical breadth of
62 knowledge, ease of transformation and hence heterologous protein expression, substrate specificity, and
63 published successes of bioproduction (Ward et al., 2018; Vickers et al., 2017). These advantages are
64 complemented by specialized synthetic biology strategies that enable tuning of ribosome binding site and
65 promoter strength, codon optimization of heterologous proteins, protein fusions, and the knocking out of
66 competing pathways. In recent years this has been accomplished by systematic gene downregulation using
67 regulatable CRISPR interference systems (Tian et al., 2019; Kim et al., 2016) that express a modified
68 dCas9 protein for fine-tuning of the overall pathway and optimization of target production. Furthermore, *E.*
69 *coli* endogenously generates isoprenoids through the MEP pathway while *S. cerevisiae* utilizes its native
70 MVA pathway, together enabling researchers to combine synthetic biological toolkits with the abundance
71 of information of these strains to facilitate high-titer isoprenoid production. As for downstream isoprenoid
72 functionalization, these metabolic chassis are genetically tractable whereas many natural isoprenoid
73 production pathways are prevalent in recalcitrant organisms that make high-titer production infeasible. Only
74 recently have certain non-model organisms been engineered to yield comparable or higher isoprenoid titers
75 than in *E. coli* and *S. cerevisiae*.
76

77 Despite the clear successes of isoprenoid production, *E. coli* and *S. cerevisiae* have significant
78 disadvantages that limit successful bioproduction at scale. Precursor limitations, either the availability of
79 IPP and DMAPP for direct synthesis of isoprenoids or the availability of MVA/MEP precursors, have been

80 identified as a major obstacle to advancing isoprenoid synthesis (Zu et al., 2020). Fine-tuning of metabolic
81 pathways within the cell to balance cofactor supply by downregulation or upregulation of select enzymes
82 has been identified as a major engineering opportunity and, although generally successful, often involves
83 strain-specific and product-guided strategies (Zu et al., 2020). Scaling of successful production is also
84 limited by the necessity of episomal expression systems, which are ill-suited for industrial production due
85 to the necessity of selective markers and their general instability.

86
87 A second major challenge in industrial isoprenoid biosynthesis is simultaneously increasing titer, rate, and
88 yield while reducing the environmental and monetary burden intrinsic to industrial production. Precursor
89 limitations are also complicated by isoprenoid production platforms that rely on sugar-based metabolism.
90 Although sugars like glucose and glycerol provide high MVA/MEP flux by generation of G3P/pyruvate or
91 acetyl-CoA, respectively, the high production costs are prohibitive to competition with petroleum derived
92 analogs. The greatest cost drivers of isoprenoid biosynthesis stem from carbon feed, which accounts for
93 over 90% of production costs, and product yield (Wu and Maravelias, 2018).

94
95 A promising solution to exorbitant substrate costs is carbon source switching, especially to carbon waste
96 streams like cellulosic biomass or C1 substrates (e.g., methane, methanol, carbon dioxide, and formate).
97 Recent estimates assert that sugar switching from glucose to pretreated cellulosic biomass could yield a
98 53% decrease in cost (Wu and Maravelias, 2018) with further gains if organisms can simultaneously
99 consume multiple substrates (e.g. hexose and pentose sugars). Growth and production on atypical carbon
100 sources and native generation of secondary metabolites is prevalent amongst many microorganisms.
101 Recent advances have capitalized on the diversity of microbial carbon assimilation pathways, especially in
102 the elucidation of synthetic and natural C1 metabolic pathways that enable access to cheap, abundant
103 carbon sources (Aldridge et al., 2021).

104
105 Many archaea have also evolved a robust array of resistance strategies to cope with inhibitory chemicals
106 and conditions. These include tolerance mechanisms (efflux pumps, heat tolerance, membrane
107 modifications, and general stress resistance) (Dunlop, 2011) that facilitate extremophilic growth in
108 inhospitable environments like anaerobic conditions or deep sea vents. These mechanisms in some cases
109 directly involve secondary metabolite production and even enable enhanced tolerance to secondary
110 metabolite toxicity (Dunlop et al., 2011). Toxicity tolerance is an appealing phenotype for biofuel production
111 systems as well as for survival on substrates that are typically toxic to many microorganisms like pretreated
112 lignocellulosic biomass (Dunlop et al., 2011). To date, bioproduction on pretreated cellulosic biomass has
113 proven challenging due to the associated toxicity of the substrate, especially the prevalence of aromatic
114 compounds. In response, researchers have begun focusing on resilient bioproduction chassis like
115 *Pseudomonas putida* and *Rhodospiridium toruloides* that can readily degrade aromatic compounds
116 (Johnson et al., 2019; Yaegashi et al., 2017).

117
118 Conversely, microbes with unique phenotypes tend to have limited metabolic toolkits available. Next
119 generation sequencing technologies have expedited exploration and characterization of novel organisms
120 from unique environments, yet direct engineering of such organisms for production remains a fundamental
121 challenge. Neither *E. coli* or *S. cerevisiae* naturally accumulate isoprenoids at high titer and bioproduction
122 is often limited to heavily modified strains with inducible episomal expression systems. Even so, the highest
123 production of isoprenoids has been achieved in *E. coli* and *S. cerevisiae* (Moser and Pichler, 2019). As a
124 result, there is a significant disparity between model and non-model isoprenoid production.

125
126 Addressing the disparity between the prevalence of nature's clever solutions to environmental challenges
127 and the genetic tractability of those organisms remains a principal obstacle in isoprenoid bioproduction. In
128 many instances, it poses the question of whether to heterologously express pathways in common metabolic

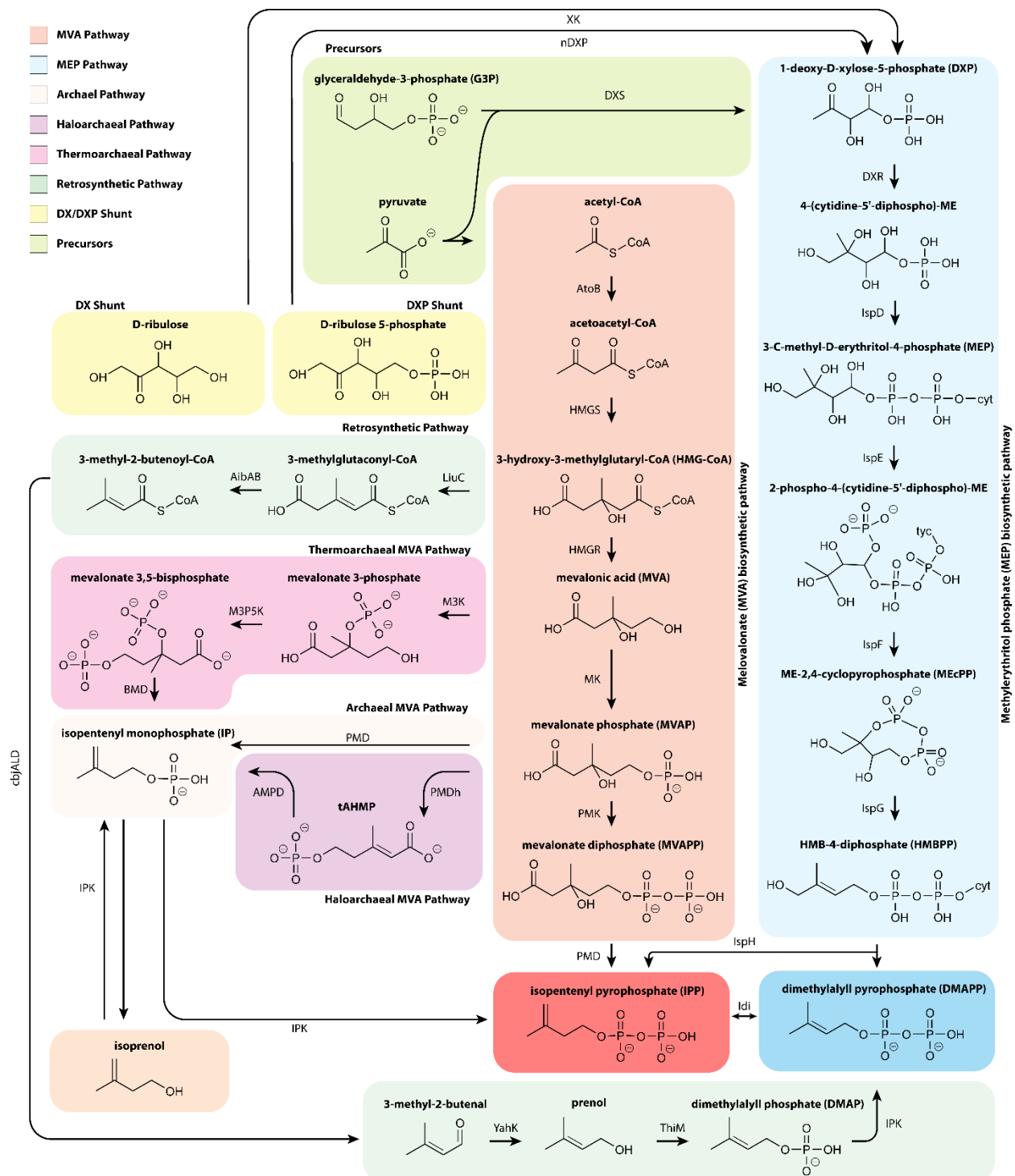
129 chassis or to optimize pathways *in situ*, both of which come with drawbacks. In this review, we highlight
130 recent advances in core understanding of isoprenoid synthesis, namely the elucidation of the archaeal MVA
131 pathways, precursor flux modulation, and how those discoveries have contributed to novel isoprenoid
132 production schemes. We then explore the exchange between lessons learned in the metabolic engineering
133 of *E. coli* and *S. cerevisiae* and of non-model microorganisms with natural predispositions for atypical and
134 economical carbon substrates. Pathways include C1 metabolism in methylophilic organisms
135 (*Methanosarcina* sp., *Methylobacterium extorquens*) and phototrophic microbes (cyanobacteria, purple non-
136 sulfur bacteria, diatoms, and green algae) capable of fixing CO₂. We also explore advances in engineering
137 of oleaginous yeast naturally capable of efficient lipid toleration and accumulation (*R. toruloides* and *Y.*
138 *lipolytica*) and finally soil bacteria with special focus on their propensity for survival on and degradation of
139 aromatic substrates (*B. subtilis* and *P. putida*). Collectively, these advances move isoprenoid biosynthesis
140 towards economic and environmental feasibility.

141

142 **Advances in isoprenoid pathway construction:**

143

144 All isoprenoids are generated from the common cellular precursors acetyl-CoA or glyceraldehyde 3-
145 phosphate (G3P) and pyruvate via either the MVA or MEP pathway, respectively (**Figure 1**). These
146 pathways share no homology and are evolutionarily distinct. Comparisons of the MVA and MEP pathway
147 efficiencies, cofactors, and energetic requirements have been well documented in previous reviews (Dugar
148 and Stephanopoulos, 2011; Yadav et al., 2012). The recent characterization of archaeal MVA pathways,
149 shunts, and alternative precursors for these pathways have harbored the development of unique and more
150 efficient routes for isoprenoid production (Kang et al., 2017; Clomburg et al., 2019; Hayakawa et al., 2018).



151
 152 **Figure 1.** A depiction of isoprenoid synthesis through the core 6 enzyme MVA and 7 enzyme MEP
 153 pathways. Also depicted are the newly discovered archaeal branches from the MVA pathway. The
 154 thermoarchaeal-type branch begins with mevalonic acid whereas the archaeal and haloarchaeal-type
 155 branches stem from MVAP. Typically, isoprenoids are synthesized by acetyl-CoA, pyruvate, and G3P,
 156 however IPP and DMAPP can also be synthesized from C5 alcohols, D-ribulose or D-ribulose-5-phosphate,
 157 and a synthetic route in which HMG-CoA is ultimately converted to prenilol. AibAB, 3-methylglutaconyl-
 158 coenzyme decarboxylase; AtoB, acetyl-CoA acetyltransferase; BMD, bisphosphomevalonate

159 decarboxylase; cbjALD, 3-methylcrotonyl-CoA reductase; DXR, 1-deoxy-D-xylulose 5-phosphate
160 reductase; DXS, 1-deoxy-D-xylulose 5-phosphate synthase; HMGR, 3-hydroxy-3-methylglutaryl-CoA
161 reductase; HMGS, 3-hydroxy-3-methylglutaryl-CoA synthase; IDI, isopentenyl diphosphate isomerase;
162 IPK, isopentenyl phosphate kinase; IspD, 2-C-methyl-D-erythritol 4-phosphate cytidyltransferase; IspE,
163 4-diphosphocytidyl-2-C-methyl-D-erythritol kinase; IspF, 2-C-methyl-D-erythritol 2,4-cyclodiphosphate
164 synthase; IspG, 4-hydroxy-3-methylbut-2-enyl diphosphate synthase; IspH, 4-hydroxy-3-methylbut-2-enyl
165 diphosphate reductase; LiuC, 3-hydroxy-3-methylglutaryl CoA dehydratase; M3K, Mevalonate 3-kinase;
166 M3P5K, Mevalonate 2-phosphate-kinase; nDXP, 1-deoxyxylulose-5-phosphate synthase; PMD,
167 phosphomevalonate decarboxylase; PMK, phosphomevalonate kinase; tAHMP, anhydromevalonate
168 diphosphate decarboxylase; ThiM, hydroxyethylthiazole kinase; XK, xylulose kinase; YahK, aldehyde
169 reductase.

170

171 **Mevalonate (MVA) pathway**

172

173 The MVA pathway is native to eukaryotes, some ancient and often predatory gram-positive bacteria
174 (Pasternak et al., 2013), as well as, with some significant deviations, archaea (Boucher et al., 2004). The
175 canonical MVA pathway commences with a Claisen condensation of two acetyl-CoA thioester molecules
176 followed by five sequential enzymatic steps that ultimately yield IPP. IPP is then converted to DMAPP by
177 the isopentenyl diphosphate isomerase (IDI) for further condensation into isoprenoid compounds.

178

179 Over the last decade, the origin of the archaeal MVA pathway - either progenating from horizontal gene
180 transfer or a cenancestor - has been hotly debated. However, recent analysis of monophylogenetic
181 candidate phyla radiation and DPANN (Diapherotrites, Parvarcheota, Aenigmarchaeota, Nanoarchaeota,
182 and Nanohaloarchaeota) have provided conclusive evidence to support an extant ancestral MVA in all
183 domains of life (Castelle and Banfield, 2018). Most notably, the archaeal pathway lacks PMK, PMD, and
184 IDI1. Instead, archaea have an alternative IDI2 similar in function to IDI1 and rely upon the recently
185 discovered isopentenyl phosphate kinase (Dellas et al., 2013) to generate IPP through unique MVA
186 intermediates. Specifically, three distinctive archaeal MVA pathways have been elucidated: the
187 haloarchaea-type MVA, the thermoplasma-type MVA, and the archaeal MVA pathway that is conserved
188 throughout the kingdom (Yoshida et al., 2020; Thomas et al., 2019; Hayakawa et al., 2018) as depicted in
189 **Figure 1**.

190

191 Beyond the perplexities of phylogenetic classification (hereditary, horizontal gene transfer, etc), the
192 elucidation of archaeal MVA pathways and their associated enzymes has proven instrumental in optimizing
193 *S. cerevisiae*/*E. coli* production titers by capitalizing upon enzyme promiscuity or efficiency. Collectively,
194 heterologous expression and fine-tuning of the MVA pathway to minimize flux bottlenecks has included the
195 expression of genes across different domains. Overexpression of HMGS and HMGR from *Staphylococcus*.
196 *aureus* (Tsuruta et al., 2009) as well as a kinase from the archaeal *M. mazei* (Primak et al., 2011), for
197 example, was successfully shown to improve C5 isoprenoid accumulation and laid the groundwork for
198 longer chain isoprenoid production via the MVA pathway (George et al., 2015).

199

200 **Methylerythritol phosphate (MEP) pathway**

201

202 The MEP pathway is native to most Gram-negative bacteria and cyanobacteria as well as to algae and
203 higher plants, but in the latter eukaryotes it is compartmentalized in the plastid. Despite being theoretically
204 more efficient than the MVA pathway, the MEP pathway is more tightly regulated and challenging to
205 engineer. Studies have elucidated rate limiting enzymatic steps in the MEP pathway, namely IDI and DXS,
206 for β -carotene production (Yuan et al., 2006). However, overexpression of MEP pathway genes can also
207 have deleterious effects on actual isoprenoid synthesis due to accumulation of intermediates. Our

208 fundamental understanding of MEP pathway regulation is incomplete, encompassing some feedback and
209 feedforward mechanisms between downstream isoprenoids and MEP intermediates (Bitok and Meyers,
210 2012). Studies in higher plants and algae, which have demonstrated that circadian light/dark cycling have
211 a significant influence on pathway regulation further complicate our understanding (Vranová et al., 2012).

212
213 A recent metabolic control analysis employed -omics studies with recombineering to show that, normalized
214 to DXS flux, IspG is the rate limiting step for isoprene synthesis with other enzymes increasing linearly with
215 DXS concentration (Volke et al., 2019). This is an important finding as isoprene is the simplest hemiterpene
216 and therefore a good reporter for MEP tuning. Yet production did not increase with overexpression of IspG
217 and IspH, suggesting instead that other cofactors may be limiting (Volke et al., 2019). Indeed, careful
218 balancing of IspG and IspH expression has shown enhanced β -carotene and α -lycopene production (Li et
219 al., 2017), suggesting that pathway tuning should be based on an intricate, product-driven approach (e.g.
220 different tuning for isoprene vs. higher chain length terpenoids) rather than an intuitive, generalizable rule.
221 In general, careful expression balancing has been the most successful strategy to MEP pathway
222 optimization due to the complexity of regulatory mechanisms in *E. coli*, though even careful balancing in
223 other organisms like the cyanobacterium *Synechococcus elongatus* has proven challenging (Englund et
224 al., 2018).

225 226 **Synthetic isoprenoid production pathways**

227
228 Although essential to isoprenoid production, high IPP and DMAPP accumulation is toxic and can result in
229 significant growth inhibition (George et al., 2018). This dilemma has led to a number of clever strategies for
230 synthetic “growth-decoupled” and “bypass” isoprenoid production routes that comprise components of
231 MVA/MEP pathways but avoid IPP/DMAPP accumulation. Many of these strategies have been informed or
232 directly use elements from the recently elucidated archaeal MVA pathways, either through direct codon
233 optimized expression or as templates for engineering promiscuous activity. A mevalonate decarboxylase
234 from *Halobacterium volcanii*, for example, was expected to demonstrate conversion of MVAP to IP and
235 employed as a template to rationally design PMDs for C5 alcohol production. The strategy successfully
236 enhanced isoprenol production by bypassing intracellular IPP accumulation (Vannice et al., 2014; Kang et
237 al., 2016). Further mutagenesis of a *S. cerevisiae* PMD in tandem with an endogenous phosphokinase
238 resulted in an IPP-bypass pathway that yields IP and ultimately the highest isoprenol titer reported at 10.8
239 g/L (Kang et al., 2017, 2019)

240
241 Retro-biosynthetic approaches postulated that archaeal IPKs could enable phosphorylation of the C5
242 alcohols (isoprenol and prenol) into IPP and DMAPP, respectively. Direct feeding of alcohols for production
243 of isoprenoid precursors could thereby decouple isoprenoid production from central carbon metabolism. Of
244 particular interest were IPKs from *Halobacterium volcanii*, *Methanothermobacter thermautotrophicus*,
245 *Thermoplasma acidophilum*, and *Methanocaldococcus jannaschii* (Chatzivasileiou et al., 2019). In one
246 study, IPKs from the latter three archaea were screened for activity and cloned into an *E. coli* strain
247 harboring a β -carotene production pathway (Liu et al., 2016). Expression of the IPK from *T. acidophilum*
248 and feeding of 2 mM prenol resulted in a 45% increase in β -carotene production and was further improved
249 by site-specific mutagenesis to 97% (Liu et al., 2016). Growth-decoupled production of lycopene was also
250 demonstrated by overexpressing a codon-optimized *T. acidophilum* IPK paired with an endogenous *E. coli*
251 phosphatase PhoN, with titers nearing 190 mg/L in an mixture of 2.5 mM prenol and isoprenol (Lund et al.,
252 2019; Clomburg et al., 2019; Chatzivasileiou et al., 2019). IPK-mediated production of carotenoid and
253 neurosporene was also improved in *E. coli* by 18-fold and 45-fold, respectively, by decoupling terpene
254 synthesis from central carbon metabolism through production on C5 alcohols (Rico et al., 2019).

255

256 Several other strategies utilize two upper MVA pathway genes (*E. coli* AtoB, *Staphylococcus aureus*
257 HMGS) prior to diverging with the expression of the hydratase LiuC and *Myxococcus xanthus*
258 decarboxylase AibAB (Clomburg et al., 2019; Eiben et al., 2020). From there, Eiben et al. demonstrated 80
259 mg/L isopentanol production through subsequent expression of *M. xanthus* AibC and *Clostridium*
260 *acetobutylicum* AdhE2 (Eiben et al., 2020). In a more holistic approach, AibAB was followed with expression
261 of the *Clostridium beijerinckii* acyl-CoA reductase (cbjALD), and *E. coli* YahK to generate prenol at the
262 highest titer reported for biological production (**Figure 1**) (Clomburg et al., 2019). Conversion of prenol to
263 DMAP was then accomplished by the *E. coli* hydroxyethylthiazole kinase (ThiM) and finally converted to
264 DMAPP by the *M. thermoautotrophicus* IPK (Clomburg et al., 2019). The unique approach employed by
265 Clomburg et al. succinctly demonstrates how novel enzymes wrought by recent discoveries can be
266 instrumental in designing pathways that circumvent metabolic bottlenecks to yield high titer production
267 platforms.

268
269 To conclude, several studies have explored novel precursors to the MEP pathway using ribulose. The initial
270 step in the MEP pathway, condensation of G3P and pyruvate with DXS, results in production of DXP with
271 the loss of a CO₂ molecule or one sixth of total carbon (Kirby et al., 2015). A D-ribulose 5-phosphate shunt
272 by nDXP was initially explored in *E. coli* by a semi-rational approach, which identified *yajO* and *ribB* gene
273 mutants as candidate enzymes and improved carbon efficiency by direct conversion of C5 sugars to C5
274 MEP intermediates. Expression of the nDXP shunt enabled a four-fold increase in MEP derived bisabolene
275 production (Kirby et al., 2015). This approach was further demonstrated in *P. putida* by expression of the
276 mutant *ribB* gene, but with low efficiency (Hernandez-Arranz et al., 2019). In an analogous work,
277 promiscuous activity of fructose-6-phosphate aldolase in *E. coli* was used to generate D-ribulose from the
278 glycolaldehyde and hydroxyacetone. Another DXP shunt overexpressed a native xylulose kinase (King et
279 al., 2017). These novel shunts, like the archaeal informed MVA pathways, have the potential to alleviate
280 precursor flux limitations. While the MVA pathway modifications have had clear success, it has yet to be
281 determined whether these shunts can address the regulatory challenges associated with MEP derived
282 isoprenoid production.

283 284 **Advances in isoprenoid functionalization**

285
286 The C5 precursors IPP and DMAPP are dephosphorylated, cyclized, and modified to create a structurally
287 diverse group of over 70,000 chemicals through a coordinated enzyme network (Kirby and Keasling, 2009;
288 Moser and Pichler, 2019). The first stage or module of isoprenoid biosynthesis is characterized by the
289 successive addition of the diphosphate precursor via head-to-head or tail-to-head condensation. The
290 second module is an operation or series of operations conducted by terpene synthases (TSs) in which the
291 terpenoid skeleton is dephosphorylated and cyclized. The third module involves further decoration by
292 cytochrome P450s (CYPs), acetyltransferases, methyltransferases, dehydrogenases, and in some cases,
293 glycosylations. This overall framework is consistently repeated in nature with some variations (Zhou and
294 Pichersky, 2020). In this section we discuss recent advances in the functionalization of isoprenoids. Broad
295 ranges of chemical production targets have been demonstrated and scaled from biofuels to
296 pharmaceuticals by heterologous expression of prenyl diphosphate synthases, TSs, and CYPs.

297 298 ***Cytochrome P450s (CYPs)***

299
300 Heme-thiolate monooxygenases or CYPs are an interesting class of enzymes that functionalize terpenes
301 through oxygenation reactions (hydroxylation, dealkylation, demethylation, decarboxylation, cyclization, C-
302 C bond cleavage, among others) and present an important opportunity for generating highly decorated
303 natural products. To date, over 300,000 CYPs have been discovered, with less than one percent actually
304 characterized (Liu et al., 2020; Li et al., 2020). There is particular interest to produce CYP-derived

305 terpenoids in microbial chassis due to the high barriers of slow growth and costly deconstruction inherent
 306 to native plant extraction.

307
 308 Engineering CYPs has significant implications for novel and unnatural bioproducts (Helfrich et al., 2019;
 309 Xiao et al., 2019). The range of oxygenated terpenes is complemented by the sheer expanse of CYP
 310 availability in plants (Zhou and Pichersky, 2020). For example, CYPs are critical for the production of
 311 bioactive molecules with high pharmacological impacts. Case studies of microbial expression include
 312 production of precursor intermediates to artemisinin (CYP71AV1, aaCPR) and taxadiene (CYP725A4,
 313 tcCPR), which are natively produced by wormwood (*Artemisia annua*) and the Pacific yew tree (*Taxus*
 314 *brevifolia*) and were heterologously expressed in *E. coli* and *S. cerevisiae*, respectively. Indeed, the diversity
 315 and complexity of plant TSs, presented elsewhere (Karunanithi and Zerbe, 2019) offer tremendous potential
 316 as candidates for microbial production.

317
 318 These specific examples demonstrate successful engineering of CYPs for pharmaceutical production,
 319 however functional plant CYP expression in microbes has proved challenging. Unfortunately, *E. coli* cannot
 320 naturally perform most posttranslational modifications and expression of membrane bound proteins like
 321 CYPs generates inclusion bodies or aggregates of insoluble proteins. The production of oxygenated
 322 taxanes in *E. coli* (Biggs et al., 2016), for example, required extensive engineering of the CYP redox-partner
 323 cytochrome P450 reductase (CPR) pairings, N-terminal modifications for better solubility, and had
 324 significant repercussions on upstream MEP pathway balance. These pairings and modifications are
 325 necessary for any heterologous CYP expression in *E. coli* and vary depending on the selected proteins.
 326 Remarkably, although yeasts are naturally capable of many posttranslational modifications, express native
 327 CPRs, and require less N-terminal modification, meta-analyses have shown that *E. coli* studies tend to have
 328 higher yield CYPs than *S. cerevisiae* despite the necessity of many more genetic modifications (Hausjell et
 329 al., 2018). Many CYP-reductase pairings have been explored in *E. coli* and *S. cerevisiae* as listed in **Table**
 330 **1**.

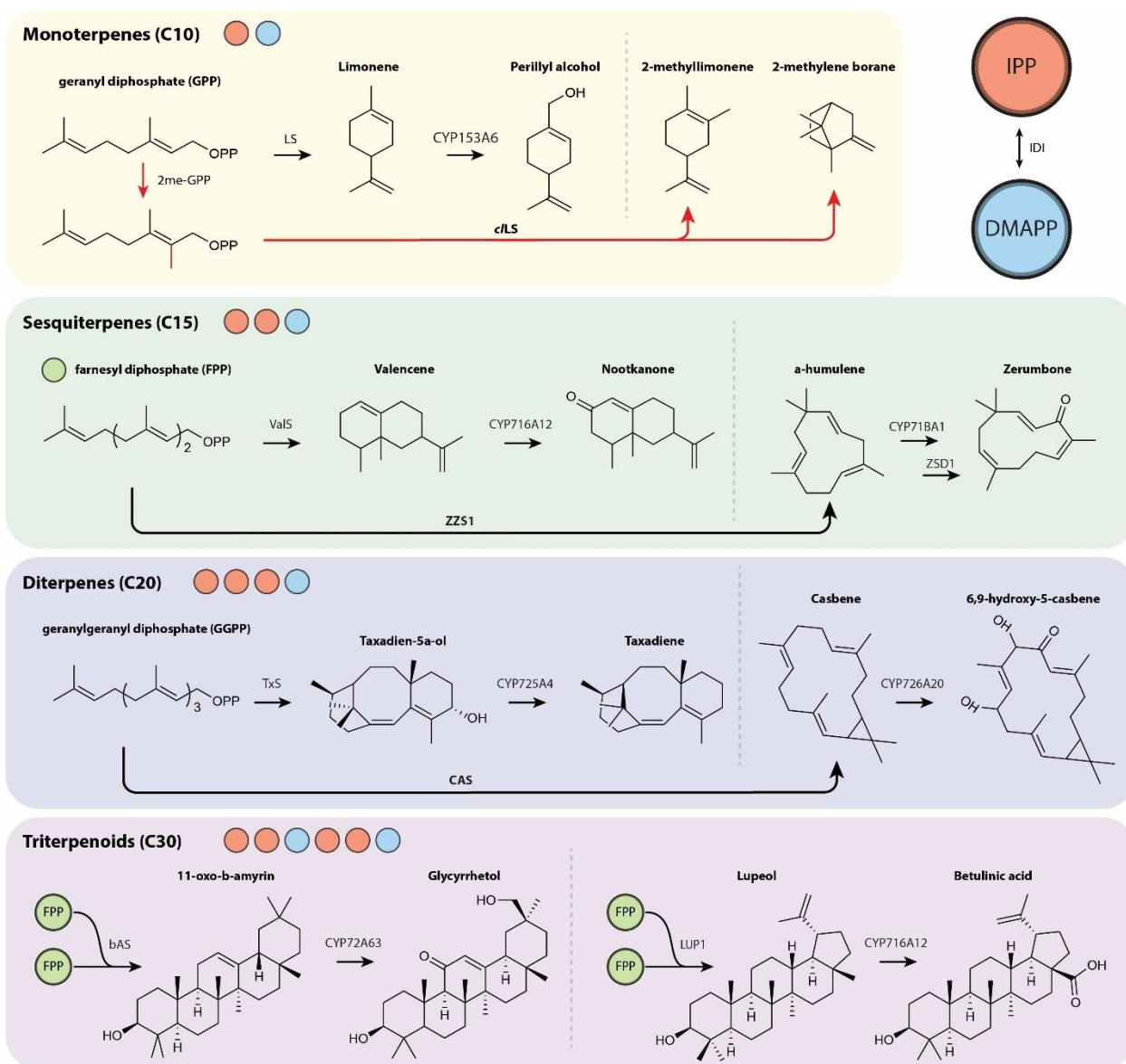
331
 332 **Table 1.** CYP expression, reductase pairing, and production of oxygenated terpenoids in various microbial
 333 hosts. Culture conditions, scale, and medium vary significantly. HPO *Hyoscyamus muticus*
 334 prenaspirodiene oxygenase; CPR, cytochrome P450 reductase.

CYP	Reductase Pair	Source organism(s)	Expression organism	Precursor	Product	Titer	Ref.
CYP71AV1	aaCPR	<i>Artemisia annua</i>	<i>S. cerevisiae</i>	Amorphadiene	Artemisinic acid	100 mg/L	(Ro et al., 2006)
CYP71AV1	aaCPR	<i>A. annua</i>	<i>E. coli</i>	Amorphadiene	Artemisinic acid	5.8 mg/L	(Chang et al., 2007)
CYP706B1	ctCPR	<i>Candida tropicalis</i>	<i>E. coli</i>	Cadinene	8-hydroxycadinene	105 mg/L	
CYP71BA1	atCPR	<i>Zingiber zerumbet</i> , <i>A. thaliana</i>	<i>E. coli</i>	α -humulene	8-hydroxy- α -humulene	2.972 μ g/L	(Yu et al., 2011)
CYP76AH1	atCPR1	<i>Salvia miltiorrhiza</i> , <i>A. thaliana</i>	<i>S. cerevisiae</i>	Miltiradiene	Ferruginol	10.5 mg/L	(Guo et al., 2013)
CYP153A6	mCPR	<i>Mycobacterium sp.</i>	<i>E. coli</i>	Limonene	Perillyl alcohol	100 mg/L	(Alonso-Gutierrez et al., 2013)
HPO	atCPR	<i>Hyoscyamus muticus</i> , <i>A. thaliana</i>	<i>P. pastoris</i>	(+)-valencene	(+)-nootkanone	208 mg/L	(Wriessnegger et al., 2014)
CYP725A4	tcCPR	<i>Taxus cuspidata</i>	<i>E. coli</i>	Paclitaxel	Oxygenated taxanes	570 mg/L	(Biggs et al., 2016)
CYP726A20	jcCPR1	<i>Jatropha curcas</i>	<i>S. cerevisiae</i>	Casbene	Oxidized casbanes	~ 1 g/L;	(Wong et al., 2018)
CYP716A12	atCPR	<i>Callitropsis nootkatensis</i> , <i>A. thaliana</i>	<i>Y. Lipolytica</i>	(+)-valencene	(+)-nootkanone	978.2 μ g/L	(Guo et al., 2018)
CYP71BA1	atCPR	<i>Z. zerumbet</i> ; <i>A. thaliana</i>	<i>S. cerevisiae</i>	α -humulene	A-humulene 8-hydroxylase; zerumbone	40 mg/L	(Zhang et al., 2018)
CYP716A12	atCPR	<i>Medicago truncatula</i> , <i>A. thaliana</i>	<i>Y. lipolytica</i>	Lupeol	Betulinic acid	26.53 mg/L	(Sun et al., 2018)
CYP716A47	pgCPR1	<i>Panax ginseng</i> , <i>A. thaliana</i>	<i>S. cerevisiae</i>	Dammarenediol II	Protopanaxidiol	11.02 g/L	(Wang et al., 2019)
CYP716A12	mtCPR	<i>M. truncatula</i>	<i>Phaeodactylum tricornutum</i>	Lupeol	Betulinic acid	0.1 mg/L	(D'Adamo et al., 2019)

BcABA1 BcABA2	bcCPR1	Botrytis cinerea	<i>S. cerevisiae</i>	FPP	Abscisic acid	4.7 mg/L	(Otto et al., 2019)
CYP72A63	atCPR1, mtCPR2, mtCPR3, guCPR2	<i>A. thaliana</i> , <i>M. truncatula</i> , <i>Glycyrrhiza uralensis</i>	<i>S. cerevisiae</i>	11-oxo-b-amyrin	Glycyrrhetol	31.8 mg/L	(Sun et al., 2020)

335
336
337
338
339
340
341
342

In recent years, microbial expression of CYPs has produced many variable length terpenoids (**Figure 2**). Of special significance are the monoterpene perillyl alcohol, an anti-cancer drug, from limonene (Alonso-Gutierrez et al., 2013) and the sesquiterpenes nootkatone, a pharmaceutical, from valencene (Guo et al., 2018) and zerumbone, an antioxidant, from α -humulene (Zhang et al., 2018). Of further interest are the pharmacologically relevant diterpenes taxadiene and oxygenated casbenes as well as triterpenoids glycyrrhetol from 11-oxo-b-amyrin and betulinic acid from lupeol.



343
344
345
346
347

Figure 2. Overview of varied length terpenoids from their diphosphate precursors (red circle, IPP; blue circle, DMAPP; green circle, FPP) with further modification by TSs and subsequent decoration by CYPs. The production of unnatural C11 monoterpenoid compounds via methyltransferase 2me-GPP is indicated with red arrows. CAS, casbene synthase; LS, limonene synthase; *c*LS, *Citrus limon* limonene synthase;

348 2me-GPP, GPP methyltransferase; TxS, taxadiene synthase; bAS, β -amyrin synthase; LUP1, lupeol
349 synthase 1; ValS, valencene synthase; ZSD1, zerumbone synthase; ZZS1, α -humulene synthase.
350

351 There have been many breakthroughs in CYP-derived terpenes in the last five years that may provide
352 guidance in the engineering of other CYP expression systems. Their interest has led to toolkits for enhanced
353 CYP selection for targeted product engineering to streamline oxyfunctionalization of terpenes (Hernandez-
354 Ortega et al., 2018). Challenges remain with regards to CYP promiscuity, enantiomeric purity, and, perhaps
355 most importantly, production titers. Hopefully, such tools will guide hypotheses and penetrate into the library
356 of known but currently inaccessible plant bioactive terpenes for use in high titer therapeutic production.
357

358 ***Atypical terpenoid production***

359
360 Several studies have investigated novel isoprenoid chain lengths through the expression of unique S-
361 adenosyl-methionine (SAM)-dependent methyltransferases that methylate the fundamental IPP/DMAPP
362 building blocks and thereby break the natural C5 dogma. In a pioneering study, a GPP methyltransferase
363 (2meGPP) from the cyanobacterium *Pseudanabaena limnetica* was expressed in *S. cerevisiae* with its
364 native 2-methylisoborneol synthase and then with seven distinct plant monoterpene synthases (Ignea et
365 al., 2018). Each synthase generated a unique fingerprint of novel C11 compounds. By demonstrating a
366 range of C11 targets, the authors provided a proof of concept for future enzyme optimization strategies
367 toward specific C11 targets. In another work, IPP SAM-dependent methyltransferases enable conversion
368 of IPP to C6 and C7 prenyl diphosphates with a methyltransferase from *Streptomyces monomycini*, which
369 could then generate C11, C16, and C17 terpenes as well as zeaxanthin-like C41, C42, and C43 compounds
370 depending on methylation (Drummond et al., 2019). A product-driven approach was also able to elucidate
371 a C-methyltransferase that generated sodoferin, an atypical C16 sesquiterpene (von Reuss et al., 2018).
372 The work demonstrated that sodoferin, which is produced naturally and perhaps exclusively by a *Serratia*
373 *plymuthica*, could be produced in *E. coli* through heterologous expression of the methyltransferase and TS
374 (von Reuss et al., 2018). A final, completely divergent approach utilizes a thiolase from lepidoptera
375 (butterflies and moths) that naturally produces juvenile hormones in the form of C16 methylated
376 diterpenoids (Eiben et al., 2019). Specifically, the thiolase PhaA condenses a propionyl-CoA with an acetyl-
377 CoA as opposed to the standard AtoB of the MVA pathway, which condenses two acetyl-CoA substrates.
378

379 It is probable that the control of specific methylation sites decreases with compound size such that targeting
380 specific triterpenoids would remain an obstacle. In the case of C11 targets, site-directed mutagenesis of
381 the monoterpene synthases did enable higher selectivity (Ignea et al., 2018), which is encouraging for future
382 engineering. These unique approaches have expanded the boundaries of isoprenoid synthesis well beyond
383 the C5 rule, though admittedly practical applications of these novel compounds have yet to be realized.
384

385 ***Meroterpenoids***

386
387 Partial isoprenoids or meroterpenoids are a class of compounds containing an isoprenoid chain paired with
388 another structure and may have beneficial bioactive properties. Broadly, meroterpenoids include cytokinins,
389 quinones, steroids, and porphyrins like heme A and chlorophyll a. The optimization of heterologous
390 meroterpenoids poses a unique engineering challenge as the isoprenoid compound must be cogenerated
391 with another structure, then converted to the terpenoid by a specified synthase.
392

393 A good case study is the production of cannabinoids in *S. cerevisiae*. Cannabinoids are of commercial
394 interest but, like many natural products, suffer from low *in planta* yields. In a recent publication, the
395 production of olivetolic acid from acetyl-CoA was engineered using a six gene pathway (Luo et al., 2019).
396 Prenylation of olivetolic acid using a *Cannabis sativa* prenyltransferase (csPT4) and further heterologous

397 synthases led to *in vivo* production of cannabigerolic acid, Δ^9 -tetrahydrocannabinolic acid, cannabidiolic
398 acid, Δ^9 -tetrahydrocannabivarinic acid, and cannabidivarinic acid (Luo et al., 2019). The work not only
399 presents a novel production scheme in *S. cerevisiae* but demonstrates the ease with which transgenic
400 elements can be translated into production chassis.

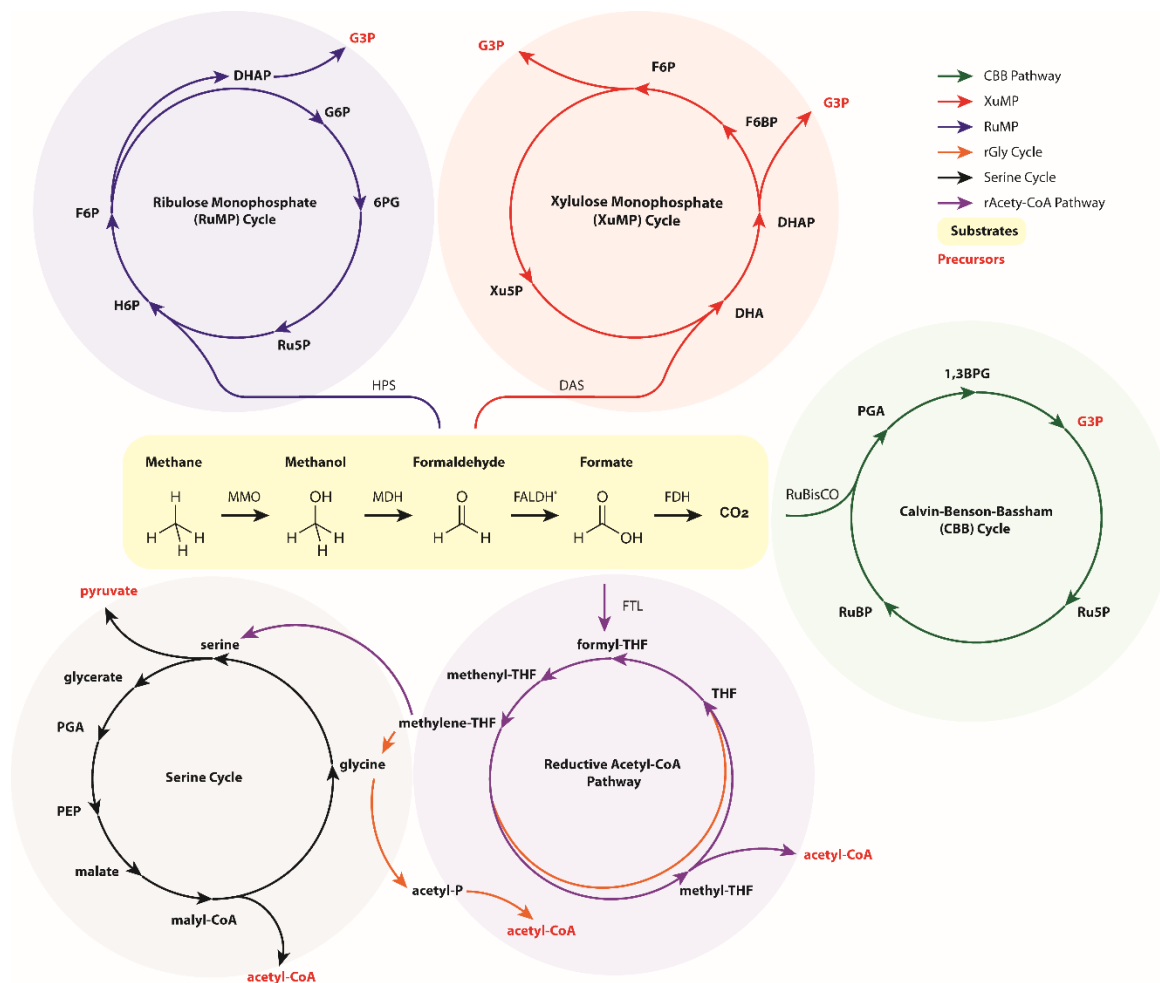
401
402 Another relevant example is the production of prenylated flavonoids, which are derived from cyclic amino
403 acid biosynthesis and can serve as nutraceuticals and medicines. They, again, are found in low natural
404 abundance in plant species like *Sophora flavescens*, a shrub and *Humulus lupulus*, brewing hops (Yang et
405 al., 2015). Production of naringenin in *S. cerevisiae* coupled with overexpression of a plant flavonoid
406 prenyltransferase enabled production of the pharmaceutically relevant 8-prenylnaringenin (Levisson et al.,
407 2019). Although both strategies were limited to yeast, they underline the flexibility of engineering
408 meroterpenoid production in microbes to address commercial needs and provide a promising opportunity
409 for accessing low abundance natural products.

410
411 Unique meroterpenoids are also generated in high natural abundance in certain microbes. Archaea differ
412 from bacteria primarily in membrane composition. Archaea produce isoprenoid-derived glycerol lipid ethers
413 (namely ester linked sn-glycerol 3-phosphates rather than ether linked sn-glycerol 1-phosphates) that
414 facilitate growth in unique environments. Full reduction of these long length C20/C40 membrane isoprenoid
415 chains is accomplished by downstream geranylgeranyl reductases (GGR). While they provide an
416 evolutionary advantage for survival in extreme conditions, membrane isoprenoids may also be utilized to
417 generate unsaturated chemicals of interest (Jain et al., 2014) . Archaeal lipids, namely archaeol and
418 caldarchaeol, have been identified as potentially valuable for the formation of archaeosomes.
419 Archaeosomes are lipid vesicles composed of archaeal derived lipids and have shown higher
420 physicochemical stability than liposomes, a conventional drug delivery system. As a result, archaeosomes
421 have been singled out as a possible adjuvant and could prove particularly valuable in slow release drug
422 delivery systems (Caforio and Driessen, 2017).

423
424 **Industrial production from C1 chemical feedstocks:**

425
426 C1 substrates are typically generated as industrial and petrochemical byproducts and, in general, C1
427 substrates are stable, abundant, and inexpensive. Advances in sequestration and hydrogenation of
428 atmospheric CO₂ via heterogeneous catalysts have enabled the conversion of emissions into valuable C₂₊
429 substrates (Ye et al., 2019). Metabolic engineering of organisms capable of C1 growth is an enticing
430 opportunity for achieving cost parity with petrochemical products while simultaneously improving
431 sustainability metrics. C1 metabolism may be subdivided into phototrophic, methylotrophic, or
432 formatrophic microbes that consume CO₂, methane/methanol, and formate/formic acid, respectively.
433 Here, we describe recent approaches for converting C1 substrates into isoprenoid precursors with specific
434 attention to works demonstrating isoprenoid production. The generalized pathways for C1 metabolism are
435 illustrated in **Figure 3**.

436



437
438

439 **Figure 3.** An amalgamated and simplified depiction of relevant C1 metabolic pathways, namely the ribulose
 440 monophosphate (RuMP) cycle, the xylulose monophosphate (XuMP) cycle, the Calvin-Benson-Bassham
 441 (CBB) cycle, the serine cycle, reductive acetyl-CoA (Wood-Ljungdahl) cycle, and the reductive glycine
 442 pathway. Intracycle reactions and conversion of metabolites by glycolysis is not shown. Emphasis is placed
 443 on precursors for isoprenoid and central carbon metabolism, namely G3P, acetyl-CoA, and pyruvate. For
 444 clarity, only the enzymes involved in the initial C1 assimilation are listed. For simplicity, FALDH is the
 445 depicted enzyme for conversion of formaldehyde to formate and the canonical methanogenic reactions are
 446 omitted. 1,3BPG, 1,3-bisphosphoglyceric acid; 6PG, 6-phosphogluconate; DAS, dihydroxyacetone
 447 synthase; DHA, dihydroxyacetone; DHAP, dihydroxyacetone phosphate; F6BP, fructose 6-bisphosphate;
 448 F6P, fructose 6-phosphate; FALDH, formaldehyde dehydrogenase; FDH, formate dehydrogenase; FTL,
 449 formate-THF ligase; G3P, glyceraldehyde 3-phosphate; G6P, glucose 6-phosphate; H6P, hexulose 6-
 450 phosphate; HPS, hexulose-6-phosphate synthase; MDH, methanol dehydrogenase; MMO, methane
 451 monooxygenase; PEP, phosphoenolpyruvate; PGA, 3-phosphoglyceric acid; Ru5P, ribulose 5-phosphate;
 452 RuBisCO, ribulose 1,5-bisphosphate carboxylase-oxygenase; RuBP, ribulose bisphosphate; THF,
 453 tetrahydrofolate; Xu5P, xylulose 5-phosphate.

454

455 **Methylotrophic isoprenoid production:**

456

457 Methane is an abundant byproduct of many chemical processes including fracking and petroleum drilling
 458 (Clomburg et al., 2017). In terms of greenhouse gas emissions, methane is approximately 20 times more

459 potent than CO₂ and excess capacity is flared at refineries, lending to an increase in direct CO₂ emissions
460 and a loss of revenue (Conrado and Gonzalez, 2014). Methane is also generated through anaerobic
461 digestion of waste biomass. To date, many successful chemical platforms utilize methane as a feedstock
462 to generate alcohols, carboxylic acids, as well as other common C2/C3 chemicals (Kuhl et al., 2012). While
463 biological conversion rates tend to be lower, certain methylotrophic organisms have arisen as potential
464 candidates to capitalize upon methane/methanol availability for more complex bioproduction. In this section,
465 we discuss recent advances in isoprenoid biosynthesis in methylotrophic cell factories across domains.
466

467 Archaea are well regarded for their ability to thrive in nutrient-limited anaerobic and extreme conditions. As
468 a result, many archaea have evolved highly efficient strategies for C1 assimilation. On one hand this has
469 helped elucidate more efficient MVA pathways as previously described, but on the other it makes the
470 engineering of tightly regulated archaeal pathways that are geared towards energy conservation
471 thermodynamically challenging. Nonetheless, one study demonstrated production of isoprene from
472 methanol in *Methanosarcina acetivorans* and *Methanosarcina barkeri* under anaerobic conditions and
473 showed a redirection of electron flux from membrane precursors in favor of isoprene accumulation (Aldridge
474 et al., 2021). The diverted isoprene accounted for 4% of total carbon flux.
475

476 More substantial success has been achieved in methylotrophic bacteria, many of which thrive in more
477 mesophilic conditions. Methylotrophic bacteria are predominantly divided into two types: Type I assimilates
478 formaldehyde using the RuMP cycle and Type II assimilates formaldehyde via the serine cycle.
479 *Methylorubrum extorquens* AM1 (formally *Methylobacterium extorquens* AM1), a Type II methylotroph, has
480 been studied for over 60 years such that many genetic tools are available (-omics data, metabolic networks,
481 genome-scale model) (Schrader et al., 2009). *M. extorquens* fermentations have produced methanol-
482 derived products ranging from 1-butanol (Hu and Lidstrom, 2014) to polymers (Orita et al., 2014). A series
483 of stepwise optimizations in *M. extorquens* AM1 included heterologous expression of the *M. xanthus* MVA
484 genes, an FPP synthase from *S. cerevisiae*, α -humulene synthase from *Zingiber zerumbet*, and reduced
485 carotenoid flux. Combinedly, these modifications resulted in the accumulation of 1.65 g/L α -humulene on
486 methanol in fed-batch cultivation, which stands as the highest titer reported (Sonntag et al., 2015). Other
487 works have explored high titer production of the MVA pathway intermediates, including 2.59 g/L mevalonic
488 acid from methanol on minimal media using a mevalonate biosensor strategy (Liang et al., 2017), which
489 suggests that high titer production of other isoprenoids is also possible. As another attractive feature, *M.*
490 *extorquens* harbors the ethylmalonyl-CoA pathway (EMCP) that includes a series of anaplerotic activated
491 CoA esters useful for pathway remodeling (Schrader et al., 2009; Schada von Borzyskowski et al., 2018).
492 Interpathway metabolite exchange has risen as a major avenue for further C1 metabolism, especially for
493 formatotrophs as discussed later.
494

495 Recently, the methylotrophic yeast *Pichia pastoris* (formally known as *Komagataella phaffii*) has arisen as
496 a promising candidate for isoprenoid production on methanol. *P. pastoris* maintains several unique
497 characteristics including a tightly regulated and highly expressed alcohol oxidase AOX1, which catalyzes
498 oxidation of methanol to formaldehyde. AOX1 is strongly induced by methanol but repressed by glucose
499 and glycerol (Hartner and Glieder, 2006). As a result, fed-batch production schemes have been designed
500 to partition high cell density growth on glycerol/glucose and production on methanol. This strategy has
501 successfully demonstrated the production of 714 mg/L lycopene (Zhang et al., 2020), (+)-ambrein, squalene
502 (Moser et al., 2018), and 208 mg/L (+)-nootkatone (Wriessnegger et al., 2014). Interestingly, the latter study
503 successfully used an approach for CYP production that had failed in *S. cerevisiae*. More involved
504 engineering of *P. pastoris* has demonstrated *de novo* production using heterologously expressed Calvin-
505 Benson-Bassham (CBB) Cycle enzymes along with native genes in the xylulose monophosphate (XuMP)
506 cycle and deletion of certain fatty acid enzymes, ultimately yielding a mutant exhibiting autotrophic growth
507 on CO₂ (Gassler et al., 2020).

508
 509 Methylo-trophic production has garnered special interest for reducing bioproduction costs either through
 510 valorization of commercial waste streams or CO₂ conversion. **Table 2** provides a list of methylo-trophic
 511 production strains, their respective C1 substrates, and product titers. In most cases, titers are significantly
 512 lower than comparative production in *E. coli* or *S. cerevisiae* and methylo-trophic cultures require significant
 513 supplementation with a rich medium that may somewhat reduce the benefits of C1 production.

514
 515 Past attempts at methylo-trophic production have historically been hindered by low carbon and energy
 516 efficiencies and addressing these issues by leveraging RuMP/Serine cycles with the CBB cycle have been
 517 long postulated (Conrado and Gonzalez, 2014). Recently, major breakthroughs in *P. pastoris* demonstrated
 518 de novo production using heterologously expressed CBB cycle enzymes, overexpressed native genes in
 519 the XuMP cycle, and deletions of certain fatty acid enzymes. The mutant was ultimately capable of
 520 autotrophic growth on CO₂ (Gassler et al., 2020). Likewise, artificial methanotrophy and formatotrophy have
 521 been explored in a complex rewiring of *E. coli* (Kim et al., 2020; Chen et al., 2020; Bennett et al., 2018).
 522 These seminal works are excellent examples of how systems biology can be applied to tune precursors,
 523 adapt strains, and incorporate well-defined isoprenoid pathways for higher production efficiency at lower
 524 substrate costs.

525
 526 **Table 2.** Production of isoprenoids by methylo-trophic organisms
 527

Organism	Feedstock	Product	Titer	Ref.
<i>Methylomonas</i> sp. 16a	Methane	astaxanthin	2.4 mg/g CDW	(Ye et al., 2007)
<i>P. pastoris</i>	Methanol**	(+)-nootkanone	208 mg/L	(Wriessnegger et al., 2014)
<i>P. pastoris</i>	Methanol**	(+)-valencene	136 mg/L	
<i>M. extorquens</i>	Methanol	a-humulene	1.65 g/L	(Sonntag et al., 2015)
<i>P. pastoris</i>	Methanol**	(+)-ambrein	105 mg/L	(Moser et al., 2018)
<i>P. pastoris</i>	Methanol**	squalene	58 mg/L	
<i>P. pastoris</i>	Methanol**	lycopene	714 mg/L	(Zhang et al., 2020)
<i>M. alcaliphilum</i>	Methane	α-humulene	0.75 mg/g CDW	(Nguyen et al., 2020)
<i>M. acetivorans</i>	Methanol*	isoprene	0.954 mM/L	(Aldridge et al., 2021)
<i>M. barkeri</i>	Methanol*	isoprene	36.0 μM/L	

528 *Complex medium

529 **Carbon sources switched from glycerol to methanol in fed-batch fermentation

530
 531 **Phototrophic isoprenoid production**
 532

533 Phototrophic growth is characterized by the photosynthetic conversion of CO₂ to sugars via complex
 534 photoreductive reactions and the Calvin-Benson-Bassham cycle. Photosynthetic organisms naturally
 535 produce carotenoids in high concentrations to cope with excess intracellular reactive oxygen species.
 536 Specifically, lutein is used in non-photochemical quenching of chlorophyll triplets during photosynthesis
 537 (Dall'Osto et al., 2006), zeaxanthin for heat dissipation and photoprotection, while carotene and chlorophyll
 538 absorb light. In many cases, gains from the engineering of the genetic architecture of photosynthesis (e.g.
 539 light harvesting complexes, RuBisCo) have been limited. Nonetheless, cyanobacteria, which only exhibit
 540 the MEP pathway, have become major targets for metabolic engineering due to their genetic plasticity and
 541 malleability with respect to isoprenoid precursors, especially through carbon sinks.

542
 543 Engineered carbon sinks operate on the hypothesis that carbon fixation reactions are faster than
 544 downstream carbon utilizing growth reactions such that the accumulation of intracellular carbon metabolites
 545 reduces NADPH consumption and ultimately inhibits photosynthesis (Oliver and Atsumi, 2015). Introduction
 546 of exogenous genes demonstrated a 1.8-fold increase in carbon yield for the generation of 2,3-butanediol

547 (Oliver and Atsumi, 2015). Others have shown sucrose, ethylene, and isobutyraldehyde production all while
548 enhancing photosynthetic activity through more optimal use of the electron transfer chain (Ducat et al.,
549 2012; Santos-Merino et al., 2021). This effect was also found to be additive when multiple sinks were
550 introduced, suggesting that “sink engineering” could be conceptually applied to secondary metabolite
551 synthesis through downstream modifications of the MEP pathway (Santos-Merino et al., 2021). Several
552 works have capitalized on this upregulation of photosynthesis by combining this source/sink approach with
553 computationally informed modification of limonene synthase, resulting in a 100-fold production
554 improvement in limonene production (Wang et al., 2016) and potential applications for other isoprenoids.
555

556 Cyanobacterial studies have also made improvements through direct modification of native isoprenoid
557 pathway genes in combination with a product-specific terminal synthase. *Synechococcus elongatus* and
558 *Synechocystis* sp. PCC 6803 have been primary targets for production with recent attempts focusing on
559 generation of isoprene, with a hallmark study demonstrating 1.26 g/L production (Yang et al., 2016; Gao et
560 al., 2016) albeit over several weeks. This feat was accomplished through the overexpression of MEP
561 pathway enzymes though, more importantly, by bioprospecting for a more efficient isoprene synthase.
562 Comprehensive analyses of the MEP pathway metabolic bottlenecks in *S. elongatus* have also been
563 studied by a systematic investigation of each enzymatic step in the MEP pathway, specifically using
564 isoprene as a simple reporter for MEP flux (Englund et al., 2018). The work found that the regulatory circuitry
565 of the *S. elongatus* MEP pathway is, like that of many other MEP pathway harboring organisms, complex
566 and that a simple overexpression of select pathway genes does not necessarily equate to higher/lower
567 production. Despite this complexity, products including squalene (Pattanaik et al., 2020), bisabolene
568 (Rodrigues and Lindberg, 2021; Sebesta and Peebles, 2020), and α -farnesene (Lee et al., 2017) have been
569 produced in *S. elongatus* through some combination of *idi*, *dxs*, *ispA* and terminal synthase overexpression.
570 It is possible that cyanobacteria could benefit from acetyl-CoA/pyruvate precursor rebalancing. In one study,
571 overexpression of a pyruvate dehydrogenase increased the pool of available acetyl-CoA for isopropanol
572 production (Hirokawa et al., 2020) and could, in theory, be applied to facilitate a heterologously expressed
573 MVA pathway or, in the reverse, to enhance pyruvate accumulation.
574

575 Unlike cyanobacteria, eukaryotic algae maintain both the MVA pathway, located in the cytosol, and the
576 MEP pathway, which is sequestered to the chloroplast in proximity to CO₂-derived metabolites from
577 photosynthesis. Algae have been hailed as candidate bioproduction microbes for many years due to their
578 propagation in many media and thus potential for growth in wastewater streams like agricultural runoff rich
579 in phosphorus and nitrogen. In general, however, eukaryotic algae are notably more challenging to engineer
580 due to their comparably smaller metabolic toolkits and robust regulatory mechanisms on metabolic flux.
581 Studies have established their propensity for some algal isoprenoid production in low titers including
582 patchoulol (Lauersen et al., 2016), bisabolene (Wichmann et al., 2018), and mixed diterpenoids (Lauersen
583 et al., 2018) in the modal alga *Chlamydomonas reinhardtii* with CO₂ as the sole carbon source. Another
584 alga, *Dunaliella salina*, has been singled out due to its resilience to highly saline environments and thereby
585 serves as a natural antibiotic against contaminants like protozoa, bacteria, dinoflagellates, and other algae.
586 *D. salina* also naturally accumulates β -carotene under abiotic stress and remains one of the few
587 commercially exploited green algae (Borowitzka, 2013; Fachet et al., 2020) along with *Haematococcus*
588 *pluvialis* for astaxanthin production. Lastly, *Botryococcus braunii*, a colonial green alga, is rich in isoprenoid
589 derived lipids that consist of 35% dry cell weight (DCW) biomass. The isoprenoids generated are
590 characterized by race and consist of either Botryococcenes (C30-C37), methylated squalenes (C31-C34),
591 or odd-number n-alkadienes or trienes (C23-C33) (Metzger and Largeau, 2005). Despite their unique
592 composition, broad attempts to culture and optimize isoprenoid production have been limited in part due to
593 slow growth comparative to other green algae (Morales-Sánchez et al., 2017). Somewhat remarkably, both
594 commercial successes stem from unmodified organisms that simply generate isoprenoids under abiotic
595 stress conditions.

596
597 Diatoms are a unique subset of algae with a characteristic cell-wall composed of silica. Certain diatoms are
598 capable of generating highly branched isoprenoids (HBIs) like trienes, tetraenes, and pentaenes intrinsic
599 to some diatoms with potential for pharmaceutical or biofuel usage (Athanasakoglou et al., 2019), possibly
600 generated by promiscuous activity of diatom specific farnesyl pyrophosphate synthases (Ferriols et al.,
601 2015). A specific diatom, *Haslea ostrearia* maintains a plastidal MEP cycle with a cytosolic MVA pathway
602 and has demonstrated significant crosstalk between these localized elements, suggesting complex
603 regulatory mechanisms perhaps in response to external stimuli and pose potential opportunities to tune
604 both pathways for downstream C5 precursor depending on target terpenoids.

605
606 A final distinctive group of phototrophic organisms are purple non-sulfur bacteria, which are identified by a
607 unique color that stems from a combination of pigmented carotenoids. In particular, *Rhodobacter*
608 *sphaeroides* is a well-established isoprenoid producer, with industrial production of sesquiterpenes
609 valencene and nootkanone demonstrated by BASF (Beekwilder et al., 2014; Schempp et al., 2018). Like
610 many bacteria, *R. sphaeroides* accumulates polyhydroxybutyrate (PHB), a biopolymer with industrial
611 bioplastic applications in of itself, under nitrogen limited conditions. Elimination of the PHB biosynthetic
612 pathway (*phaC1*, *phaC2*) and expression of the heterologous MVA pathway contributed to increased flux
613 through the isoprenoid pathway under nitrogen limited conditions (Orsi et al., 2020b).

614
615 As a whole, photosynthetic organisms remain tantalizingly elusive for high titer heterologous isoprenoid
616 production despite advances in “sink engineering” and successes in the production of certain short chain
617 biofuels.

618 **Formatotrophic production pathways**

619
620 Formate remains an enticing C1 substrate due to the relative ease with which it may be generated.
621 Proposed strategies include the hydration of syngas, the hydrogenation of CO₂, and electrochemical
622 reduction of CO₂ using, preferably, renewable generated electricity (Yishai et al., 2016). Bioproduction on
623 formate remains challenging, though recent works have attempted to address this challenge by mapping
624 natural pathways within the context of microbial metabolism (Bar-Even, 2016). The intrinsic nature of
625 formate as an intermediate and availability of natural formate assimilation pathways like the serine,
626 reductive acetyl-CoA, RuMP, XuMP, and reductive glycine pathways have led to the proposal of many
627 synthetic pathways that could theoretically outperform their natural counterparts (Bar-Even, 2016). This
628 hypothesis was encouraged by a previous study that determined formate, not formaldehyde, was the major
629 branch point in *M. extorquens* methylotrophy (Crowther et al., 2008). In particular, this suggested that direct
630 feeding of formate could be energetically beneficial due to the affiliated reduction of NAD⁺ in aldehyde
631 dehydrogenase thereby further supporting formatotrophic pathways (Crowther et al., 2008).

632
633
634 Acting on this hypothesis, *M. extorquens* genes encoding formate-THF ligase, methenyl-THF
635 cyclohydrolase, and methylene-THF dehydrogenase were heterologously expressed in *E. coli* to enable
636 growth on formate through the serine cycle. In combination with downstream modifications, the strain was
637 capable of 90 mg/L ethanol production on sugar-free formate minimal medium by adaptive laboratory
638 evolution (ALE) (Kim et al., 2019). In a subsequent study, expression of the reductive glycine pathway
639 (rGlyP) in *E. coli* enabled growth on methanol and formate (Kim et al., 2020). Despite clear demonstration
640 of formate-based growth here and *M. extorquens* isoprenoid production on methanol above, few formate
641 derived isoprenoid compounds have been shown. A single exception was a study of the archaea
642 *Methanococcus maripaludis*, which is capable of growth on H₂, CO₂, formate, and acetate as substrates
643 under strict anaerobic conditions. Heterologous expression of a geraniol synthase enabled production of
644 4.0 mg/g and 2.8 mg/g geraniol on H₂/CO₂ and formate feeds, respectively (Lyu et al., 2016). Although

645 meager, this represents a baseline for further isoprenoid production and, with the addition of the
646 groundbreaking production of formatotrophic *E. coli* works, likely represents the first of many formate-based
647 production strains.

648
649 So far, we have described a number of routes for isoprenoid production on C1 substrates, including several
650 instances in which whole pathways have been translated between organisms. Life cycle assessment (LCA)
651 and techno-economic analysis (TEA) will both be critical in quantifying the relative process level
652 sustainability and monetary impacts, validating whether modified microbes are competitive with
653 conventional production on glucose or from petroleum, and prioritizing future optimization opportunities
654 based on projected impact gains. Growth and production on C1 substrates are inherently more sustainable
655 than on pure sugar substrates, however the sustainability of the entire process from cradle-to-gate will be
656 contingent on nontrivial improvement of production titer, rate, and yield. While LCAs and TEAs are common
657 in CO₂-derived biofuel production, they remain uncommon for all other C1 substrates. Indeed, the first
658 LCA/TEA of a methane-derived bioproduct was only recently published (Fei et al., 2020). Nonetheless this
659 initial study provides a baseline for future valorization of other C1-derived chemicals and, hopefully,
660 represents a first effort to quantify the economic and sustainability advantages of C1 substrates.

661 **Isoprenoid production on lignocellulosic carbon sources**

662
663 Certain microbes are capable of valorizing more complex waste streams due to unique evolutionary
664 predispositions. Here, we describe two strains of oleaginous yeasts, *Yarrowia lipolytica* and
665 *Rhodospiridium toruloides*, capable of high titer isoprenoid production from woody biomass and waste
666 cooking oil (WCO). Lastly, we describe two prototypical isoprenoid production platforms: *P. putida*, which
667 is a prime candidate for conversion of pretreated lignocellulosic biomass, and *B. subtilis*, a candidate
668 bacteria renown for high titer protein production.

669 ***Yarrowia lipolytica***

670
671 The oleaginous yeast *Yarrowia lipolytica* can naturally assimilate many atypical carbon sources including
672 glycerol, organic acids, succinate, citrate, and even WCO. Likewise, *Y. lipolytica* is of keen interest due to
673 its natural accumulation of β -carotene, farnesene, and linalool. Multi-copy pathway integration has proven
674 especially successful in targeted isoprenoid overproduction (Xie et al., 2015). A recent work applied a
675 random chromosomal integration approach of multiple MVA pathway operons, cofactor modulation, and
676 culture condition tuning produced 25.55 g/L α -farnesene on YPD complex medium over 20 days in fed-
677 batch production with significant byproduct formation (Liu et al., 2019). A similar strategy led to 6.5 g/L
678 production of β -carotene by chromosomal integration of multiple copies of CarB, CarRP, and GGPPS in
679 fed-batch production with over 40 g/L lipid byproduct (Larroude et al., 2018). Other reports of note include
680 high squalene production at titers of 531.6 mg/L (Gao et al., 2017) and 402.4 mg/L (Arnesen et al., 2020).
681 Building upon previous limonene demonstrations with neryl diphosphate synthase (tNPPS1) from
682 *Agastache rugosa* (Korean mint) and limonene synthase from *Solanum lycopersicum* (tomato) (Cao et al.,
683 2016), *Y. lipolytica* ultimately yielded 165.3 mg/L limonene on glycerol/citrate (Cheng et al., 2019). More
684 comprehensive descriptions of *Y. lipolytica* regulatory changes for production have also been published
685 (Arnesen et al., 2020).

686
687 *Y. lipolytica* is also capable of converting fatty acids into C2 substrates through the beta-oxidation pathway
688 and has high native lipid tolerance. Recent works have demonstrated high lipid production of modified *Y.*
689 *lipolytica* on pretreated lignocellulosic biomass (0.11 g lipids/g sugars), even approaching efficiencies
690 observed on glucose (Yook et al., 2020). In fact, *Y. lipolytica* has shown up to 90% DCW lipid accumulation
691 (Park et al., 2018), which demonstrates an encouraging propensity for lipid tolerance. This tolerance has
692
693

694 been harnessed by works that have grown *Y. lipolytica* strains on WCO. Growth on WCO increased lipolytic
695 activity (Domínguez et al., 2010) and, in one study, a *Y. lipolytica* strain expressed D-limonene synthase
696 (*Citrus limon*) and L-limonene synthase (*Mentha spicata*) to yield 2.4 mg/L of each enantiomer on WCO
697 (Pang et al., 2019). Although this strain has produced only 11 mg/L of each enantiomer on complex medium,
698 this stands as an excellent proof of concept for future ALE and optimization studies on WCO.

699
700 Xylose catabolism and overcoming catabolite repression are major boundaries to bioproduction on
701 lignocellulosic biomass (Sun et al., 2021). One study showed that carbon source switching enabled
702 production of 20.6 mg/L and 15.1 mg/L limonene in *Y. lipolytica* from xylose and a 50% lignocellulosic
703 biomass 50% YP rich medium broth, respectively (Yao et al., 2020). This feat was accomplished by
704 overexpression of a native xylulose synthase with heterologous expression of xylitol dehydrogenase and
705 xylulose reductase from *Scheffersomyces stipitis* (Yao et al., 2020). Together, these modifications provided
706 increased G3P production and, ultimately, increased flux through the MVA pathway.

707 708 ***Rhodospiridium toruloides***

709
710 *R. toruloides* has attracted attention due to natural high titer lipid and carotenoid accumulation, namely
711 torularhodin, torulene, γ -carotene, and β -carotene, as a convenient carbon storage mechanism under
712 nitrogen-limited conditions (Park et al., 2018). Originally isolated from wood pulp, *R. toruloides* can also
713 metabolize many components of lignocellulosic biomass and has shown simultaneous uptake not only of
714 pentose and hexose sugars, but of p-coumaric acid and aromatic motifs analogous to lignin, which suggest
715 that it could be adapted for direct consumption of lignin (Yaegashi et al., 2017). These traits are further
716 complemented by its ability to thrive on various pretreatment conditions. For example, growth has been
717 demonstrated on ionic liquid (choline α -ketoglutarate) and alkaline pretreated cellulosic biomass, with the
718 latter accumulating 680 mg/L α -bisabolene in fed-batch reactor conditions (Yaegashi et al., 2017). Further
719 optimization of the α -bisabolene synthase cassette yielded 4-fold increased titer on lignocellulosic biomass,
720 reaching a final titer of 2.2 g/L on corn stover hydrolysate (Kirby et al., 2021). 1,8-cineole was also
721 accumulated to a titer of 1.4 g/L on the same substrate, both of which represent titers that, even without
722 significant core metabolic rewiring or downregulation, outstrip comparative *E. coli* and *S. cerevisiae*
723 production. Importantly, pilot scaling of *R. toruloides* to a 1000 L bioreactor for lipid production has been
724 successfully shown (Soccol et al., 2017). Collectively, these traits establish *R. toruloides* as a potential
725 microbial host for lignin valorization. The translation of successful pilot scale *R. toruloides* lipid production
726 platforms to strains with tuned lipid reflex pathways could elevate the yeast to an industrially competitive
727 isoprenoid production platform.

728 729 ***Pseudomonas putida***

730
731 As noted with *Y. lipolytica*, tolerance to and simultaneous uptake of multiple carbon substrates is a key
732 phenotype for successful bioproduction on lignocellulosic biomass. The soil bacterium *Pseudomonas*
733 *putida* maintains significant advantages over common production chassis due to its natural biodegradation
734 pathways and oxidative stress tolerance, which has contributed to its broad proliferation in many
735 environmental niches. Several studies have explored substrate tolerance through toxicity adaptive
736 laboratory evolution (TALE) of *P. putida* (Lim et al., 2021; Mohamed et al., 2020). A recent work integrated
737 three different xylose pathways (Dahms, Isomerase, and Weimberg) on plasmids to enable growth on
738 xylose, a prominent component of degraded hemicellulose (Bator et al., 2019). The combination of pathway
739 expression and ALE resulted in improved tolerance and hence improved growth rate (Bator et al., 2019)

740
741 Other production schemes have exploited the natural aromatic tolerance of *P. putida* for growth on
742 substrates like toluene, m-xylene, and p-xylene (Nikel and de Lorenzo, 2018). Comparatively, *P. putida*

743 maintains better *de novo* tolerance towards products that are typically toxic to other organisms (Mi et al.,
744 2014). For example, the saprophytic uptake of organic nutrients and high tolerance to oxidative stress is
745 ideal for biofuel production candidates (Kim and Park, 2014). These traits coupled with overexpression of
746 efflux pumps have shown increased tolerance to short chain C4 and C5 alcohols, which could prove
747 especially valuable for production of isoprenoid biofuels (Basler et al., 2018).
748

749 In a hallmark bioproduction study, 2.21 g/L of mevalonate were generated by *P. putida* in M9 minimal
750 medium supplemented with 7.5 g/L 2,3-butanediol by overexpression of the upper MVA pathway enzymes,
751 namely the native AtoB and the MvaE/MvaS from *Enterococcus faecalis* (Yang et al., 2020). Mevalonate
752 production on 2,3-butanediol proved 6.61- and 8.44-fold higher than production on glucose and glycerol,
753 respectively, though with manageable growth inhibition (Yang et al., 2020). Overall, *P. putida* isoprenoid
754 production has historically been limited to zeaxanthin and geranic acid such that only recently have studies
755 begun addressing MEP/heterologous MVA precursor limitations. One such study exhibited metabolic
756 rerouting of central carbon metabolism from the EMP to ED cycles for better precursor management,
757 namely efficient pyruvate production (Sánchez-Pascuala et al., 2019). This strategy led to a 2-fold increase
758 in carotenoid yield on glucose with plasmid expression of a lycopene synthesis pathway but without any
759 modification to the endogenous MEP pathway (Sánchez-Pascuala et al., 2019).
760

761 It is clear that *P. putida* has high innate tolerance to toxic substrates and, as in nature, can adapt to adverse
762 growth conditions. The next, critical stages of realizing *P. putida* as a chemical production platform will be
763 combining advances in ALE, precursor availability, and pathway tuning to enhance terpene synthesis on
764 atypical carbon substrates.
765

766 ***Bacillus subtilis***

767

768 *Bacillus subtilis* is one of the best characterized gram-positive bacteria to date and has been an attractive
769 bioproduction candidate due to high titer protein production and high secreting properties. Largely, the
770 industrial focus has been on the production of biologics and enzymes (Pham et al., 2019). *B. subtilis*
771 maintains a faster growth rate than *S. cerevisiae*, a robust metabolism on diverse carbon substrates, and
772 has also shown natural isoprene production at titers comparable to *E. coli* (Zhang et al., 2015). Unlike other
773 chassis organisms like *P. putida*, *B. subtilis* is generally recognized as safe (GRAS), a designation that
774 reduces regulatory boundaries to commercialization. Collectively, these factors suggest that *B. subtilis*
775 could be an excellent candidate for isoprenoid production. Unfortunately, production studies remain
776 relatively limited in part due to a poorly defined metabolic toolkit, which has historically been hampered by
777 a limited subset of selection/countersselection markers that have made genetic manipulation challenging.
778

779 Mirroring in *E. coli* from the early 2000s, recent production studies demonstrated that incorporation of
780 amorphaadiene synthase (ADS) with overexpression of DXS and IDI led to the accumulation of 20 mg/L
781 amorphaadiene (Zhou et al., 2013). This titer has dramatically improved to 116 mg/L using a CRISPR-cas9
782 system without culture medium optimization (Song et al., 2021) and then to 416 mg/L (Pramastya et al.,
783 2021) with pyruvate supplementation. Another recent study overexpressed the entire MEP pathway
784 excluding IDI, a taxadiene synthase, and a heterologous GGPPS in *B. subtilis*, leading to an accumulation
785 of 17.8 mg/L taxadiene (Abdallah et al., 2019). Expression of a squalene synthase from *Bacillus*
786 *megaterium* also enabled 7.5 mg/L production of squalene, which can serve as a precursor to other
787 triterpenoids (Song et al., 2020). Although far from competitive with *E. coli* and *S. cerevisiae*, these initial
788 demonstrations have provided a basis of isoprenoid production in *B. subtilis*. The publication by Song et al.
789 is of particular interest due to their application of CRISPR-cas9 to circumvent boundaries that have
790 historically limited the establishment of *B. subtilis* as an isoprenoid production workhorse. In theory, this
791 approach could be easily translated to the production of other isoprenoid targets.

792
793
794

Perspectives and Conclusion

795 The rapid expansion of -omics studies, deep sequencing, and pathway engineering have facilitated
796 bioprospecting of more efficient enzymes, robust combinatorial approaches for tailored isoprenoid
797 production, and the design of altogether novel production pathways. Such tools have also facilitated the
798 exploration of plant derived CYPs and terminal synthases whose subsequent expression has expanded the
799 microbial isoprenoid repertoire to more pharmacologically relevant as well as entirely synthetic terpenoids.
800 In this review, we focused on improvements to isoprenoid precursor biosynthesis and translation of
801 enzymes or pathways between organisms, which could assist in overcoming current major barriers to
802 commercial viability (Zu et al., 2020). Specifically, we highlighted how atypical carbon sources and non-
803 model organisms harbor metabolic advantages that could be harnessed to reduce substrate costs and the
804 associated emissions of bioproduction. Co-substrate utilization by certain organisms as in the case of *R.*
805 *toruloides* and *P. putida* has the potential to unlock lignocellulosic biomass and many methylotrophs could
806 tap into inexpensive and highly abundant substrates.

807
808 We have also described works that capitalized upon the modularity of isoprenoid advances through
809 heterologous expression of entire pathways. Systems engineering strategies are of particular interest for
810 C1 metabolism. The translation of successful whole systems engineering strategies from *E. coli* and *S.*
811 *cerevisiae* to non-model organisms will prove useful in further optimization. For example, the entire MVA
812 pathway had been expressed in *E. coli* many years ago (Martin et al., 2003) and a decade later, the entire
813 MEP pathway has been expressed in *S. cerevisiae* conversely (Kirby et al., 2016). Both strains have also
814 been extensively mapped through metabolic flux analysis (MFA) which has proven pivotal in metabolic
815 engineering (Orth et al., 2010). The translation of systems engineering strategies like MFA and genome-
816 scale modeling to other organisms will undoubtedly help to inform and improve isoprenoid production in
817 non-model organisms. An MFA of *R. sphaeroides*, for example, showed a mutualistic coupling between its
818 MEP and MVA pathways (Orsi et al., 2020a). Remarkably the true extent of the MEP pathway - MVA
819 pathway relationship could not be resolved as gene knockouts tended to have unpredictable effects on C13
820 product partitioning but suggested complex regulatory interactions. Nonetheless further work could shed
821 light on how such combined MVA/MEP pathway systems could prove beneficial (Orsi et al., 2020a).
822 Similarly, a metabolic flux reconstruction of *Dunaliella salina* established baseline carbon metabolism
823 during carotenogenesis (Fachet et al., 2020), a critical step in elucidating metabolic bottlenecks. TALE has
824 also proven a powerful strategy for increasing resistance to toxicity of high titer products especially with
825 alcohols. TALE has now been applied to *P. putida* and enhanced toxicity tolerance against the
826 lignocellulosic aromatics such as p-coumaric acid and ferulic acid (Mohamed et al., 2020)(Lim et al., 2020).
827 The application of machine learning approaches has enabled extrapolation and gap filling in genome-scale
828 models for rationally designed engineering strategies of non-canonical organisms, as demonstrated to great
829 effect in *Y. lipolytica* (Czajka et al., 2021). And, finally, C1 assimilation pathways have been thoroughly
830 explored, synthetic and natural routes hypothesized (Bar-Even, 2016), then optimal pathways have been
831 heterologously expressed in conventional production chassis (Kim et al., 2020). Having shown adapted
832 growth on C1 substrates there is now a tremendous opportunity to further develop strains for isoprenoid
833 production especially given the comparative sustainability and cost reduction of such substrates with
834 respect to production on refined sugars.

835
836 Consortial approaches have also proven valuable by improving total system productivity. Microbial
837 consortia have proven successful for short chain alcohol production from lignocellulosic biomass (Minty et
838 al., 2013) and have recently been explored in the cross-feeding of methane-derived organic acids produced
839 by *Methylococcus capsulatus* to *E. coli* for the generation of mevalonate at 60 mg/L (Lee et al., 2021).
840 Building upon CYP optimization, an *E. coli* and *S. cerevisiae* consortium produced 33 mg/L oxygenated

841 taxanes in a consortia where *E. coli* consumes xylose and produces acetate and the precursor taxadiene
842 for consumption and further conjugation in *S. cerevisiae*, respectively (Zhou et al., 2015). Another group
843 produced 0.32 g mevalonate/g ethanol in *P. putida* batch experiments (Yang et al., 2019) that, paired with
844 the aforementioned successes in ALE, could provide another promising cross-feeding consortial
845 bioproduction strategy. Finally, isoprenoid production has been expanded to 2,3-butanediol (Yang et al.,
846 2020), which could facilitate consortial bioproduction by subdividing pathways between members

847
848 Exploration of the microbial tree of life has continued to yield an abundant natural diversity of protein
849 homologues, pathway shunts, and mechanisms with which targeted production of isoprenoids has been
850 demonstrably improved. The principal challenge of isoprenoid bioproduction in the next decade will be
851 bridging the knowledge gap between conventional high titer bioproduction on pure sugar substrates and
852 non-model comparatively low titer production on affordable substrates.

853

854

855 **Conflict of interest statement**

856

857 The authors declare that they have no known competing financial interests or personal relationships that
858 could have appeared to influence the work reported in this paper.

859

860

861 **Acknowledgements**

862

863 This work was supported by the DOE Joint BioEnergy Institute (<http://www.jbei.org>), supported by the US
864 Department of Energy, Office of Science, Office of Biological and Environmental Research, through contract
865 DE-AC0205CH11231 with Lawrence Berkeley National Laboratory. The United States Government retains
866 and the publisher, by accepting the article for publication, acknowledges that the United States Government
867 retains a non-exclusive, paid-up, irrevocable, worldwide license to publish or reproduce the published form
868 of this manuscript, or allow others to do so, for United States Government purposes. The views and opinions
869 of the authors expressed herein do not necessarily state or reflect those of the United States Government
870 or any agency thereof. Neither the United States Government nor any agency thereof, nor any of their
871 employees, makes any warranty, expressed or implied, or assumes any legal liability or responsibility for
872 the accuracy, completeness, or usefulness of any information, apparatus, product, or process disclosed, or
873 represents that its use would not infringe privately owned rights.

874 **Bibliography**

- 875
- 876 Abdallah, I. I., Pramastya, H., van Merkerk, R., Sukrasno, and Quax, W. J. (2019). Metabolic Engineering
877 of *Bacillus subtilis* Toward Taxadiene Biosynthesis as the First Committed Step for Taxol
878 Production. *Front. Microbiol.* 10, 218. doi:10.3389/fmicb.2019.00218.
- 879 Aldridge, J., Carr, S., Weber, K. A., and Buan, N. R. (2021). Anaerobic production of isoprene by
880 engineered methanosarcina species archaea. *Appl. Environ. Microbiol.* 87.
881 doi:10.1128/AEM.02417-20.
- 882 Alonso-Gutierrez, J., Chan, R., Bath, T. S., Adams, P. D., Keasling, J. D., Petzold, C. J., and Lee, T. S.
883 (2013). Metabolic engineering of *Escherichia coli* for limonene and perillyl alcohol production.
884 *Metab. Eng.* 19, 33–41. doi:10.1016/j.ymben.2013.05.004.
- 885 Arnesen, J. A., Kildegaard, K. R., Cernuda Pastor, M., Jayachandran, S., Kristensen, M., and Borodina, I.
886 (2020). *Yarrowia lipolytica* Strains Engineered for the Production of Terpenoids. *Front. Bioeng.*
887 *Biotechnol.* 8, 945. doi:10.3389/fbioe.2020.00945.
- 888 Athanasakoglou, A., Grypioti, E., Michailidou, S., Ignea, C., Makris, A. M., Kalantidis, K., Massé, G.,
889 Argiriou, A., Verret, F., and Kampranis, S. C. (2019). Isoprenoid biosynthesis in the diatom
890 *Haslea ostrearia*. *New Phytol.* 222, 230–243. doi:10.1111/nph.15586.
- 891 Bar-Even, A. (2016). Formate assimilation: the metabolic architecture of natural and synthetic pathways.
892 *Biochemistry* 55, 3851–3863. doi:10.1021/acs.biochem.6b00495.
- 893 Basler, G., Thompson, M., Tullman-Ercek, D., and Keasling, J. (2018). A *Pseudomonas putida* efflux
894 pump acts on short-chain alcohols. *Biotechnol Biofuels* 11, 136. doi:10.1186/s13068-018-1133-9.
- 895 Bator, I., Wittgens, A., Rosenau, F., Tiso, T., and Blank, L. M. (2019). Comparison of three xylose
896 pathways in *Pseudomonas putida* KT2440 for the synthesis of valuable products. *Front. Bioeng.*
897 *Biotechnol.* 7, 480. doi:10.3389/fbioe.2019.00480.
- 898 Beekwilder, J., van Houwelingen, A., Cankar, K., van Dijk, A. D. J., de Jong, R. M., Stoop, G.,
899 Bouwmeester, H., Achkar, J., Sonke, T., and Bosch, D. (2014). Valencene synthase from the
900 heartwood of Nootka cypress (*Callitropsis nootkatensis*) for biotechnological production of
901 valencene. *Plant Biotechnol. J.* 12, 174–182. doi:10.1111/pbi.12124.
- 902 Bennett, R. K., Gonzalez, J. E., Whitaker, W. B., Antoniewicz, M. R., and Papoutsakis, E. T. (2018).
903 Expression of heterologous non-oxidative pentose phosphate pathway from *Bacillus*
904 *methanolicus* and phosphoglucose isomerase deletion improves methanol assimilation and
905 metabolite production by a synthetic *Escherichia coli* methylotroph. *Metab. Eng.* 45, 75–85.
906 doi:10.1016/j.ymben.2017.11.016.
- 907 Biggs, B. W., Lim, C. G., Sagliani, K., Shankar, S., Stephanopoulos, G., De Mey, M., and Ajikumar, P. K.
908 (2016). Overcoming heterologous protein interdependency to optimize P450-mediated Taxol
909 precursor synthesis in *Escherichia coli*. *Proc. Natl. Acad. Sci. USA* 113, 3209–3214.
910 doi:10.1073/pnas.1515826113.
- 911 Bitok, J. K., and Meyers, C. F. (2012). 2C-Methyl-d-erythritol 4-phosphate enhances and sustains
912 cyclodiphosphate synthase IspF activity. *ACS Chem. Biol.* 7, 1702–1710.
913 doi:10.1021/cb300243w.
- 914 Borowitzka, M. A. (2013). High-value products from microalgae—their development and
915 commercialisation. *J Appl Phycol* 25, 743–756. doi:10.1007/s10811-013-9983-9.
- 916 Boucher, Y., Kamekura, M., and Doolittle, W. F. (2004). Origins and evolution of isoprenoid lipid
917 biosynthesis in archaea. *Mol. Microbiol.* 52, 515–527. doi:10.1111/j.1365-2958.2004.03992.x.
- 918 Caforio, A., and Driessen, A. J. M. (2017). Archaeal phospholipids: Structural properties and biosynthesis.
919 *Biochim. Biophys. Acta Mol. Cell Biol. Lipids* 1862, 1325–1339. doi:10.1016/j.bbalip.2016.12.006.
- 920 Cao, X., Lv, Y.-B., Chen, J., Imanaka, T., Wei, L.-J., and Hua, Q. (2016). Metabolic engineering of
921 oleaginous yeast *Yarrowia lipolytica* for limonene overproduction. *Biotechnol Biofuels* 9, 214.
922 doi:10.1186/s13068-016-0626-7.

923 Castelle, C. J., and Banfield, J. F. (2018). Major new microbial groups expand diversity and alter our
924 understanding of the tree of life. *Cell* 172, 1181–1197. doi:10.1016/j.cell.2018.02.016.

925 Chang, M. C. Y., Eachus, R. A., Trieu, W., Ro, D.-K., and Keasling, J. D. (2007). Engineering *Escherichia*
926 *coli* for production of functionalized terpenoids using plant P450s. *Nat. Chem. Biol.* 3, 274–277.
927 doi:10.1038/nchembio875.

928 Chappell, J. (1995). The biochemistry and molecular biology of isoprenoid metabolism. *Plant Physiol.*
929 107, 1–6. doi:10.1104/pp.107.1.1.

930 Chatzivasileiou, A. O., Ward, V., Edgar, S. M., and Stephanopoulos, G. (2019). Two-step pathway for
931 isoprenoid synthesis. *Proc. Natl. Acad. Sci. USA* 116, 506–511. doi:10.1073/pnas.1812935116.

932 Chen, F. Y.-H., Jung, H.-W., Tsuei, C.-Y., and Liao, J. C. (2020). Converting *Escherichia coli* to a
933 Synthetic Methylothermophilic Growing Solely on Methanol. *Cell* 182, 933–946.e14.
934 doi:10.1016/j.cell.2020.07.010.

935 Cheng, B.-Q., Wei, L.-J., Lv, Y.-B., Chen, J., and Hua, Q. (2019). Elevating Limonene Production in
936 Oleaginous Yeast *Yarrowia lipolytica* via Genetic Engineering of Limonene Biosynthesis Pathway
937 and Optimization of Medium Composition. *Biotechnol. Bioprocess Eng.* 24, 500–506.
938 doi:10.1007/s12257-018-0497-9.

939 Clomburg, J. M., Crumbley, A. M., and Gonzalez, R. (2017). Industrial biomanufacturing: The future of
940 chemical production. *Science* 355. doi:10.1126/science.aag0804.

941 Clomburg, J. M., Qian, S., Tan, Z., Cheong, S., and Gonzalez, R. (2019). The isoprenoid alcohol
942 pathway, a synthetic route for isoprenoid biosynthesis. *Proc. Natl. Acad. Sci. USA* 116, 12810–
943 12815. doi:10.1073/pnas.1821004116.

944 Conrado, R. J., and Gonzalez, R. (2014). Chemistry. Envisioning the bioconversion of methane to liquid
945 fuels. *Science* 343, 621–623. doi:10.1126/science.1246929.

946 Crowther, G. J., Kosály, G., and Lidstrom, M. E. (2008). Formate as the main branch point for
947 methylothermophilic metabolism in *Methylobacterium extorquens* AM1. *J. Bacteriol.* 190, 5057–5062.
948 doi:10.1128/JB.00228-08.

949 Czajka, J. J., Oyetunde, T., and Tang, Y. J. (2021). Integrated knowledge mining, genome-scale
950 modeling, and machine learning for predicting *Yarrowia lipolytica* bioproduction. *Metab. Eng.* 67,
951 227–236. doi:10.1016/j.ymben.2021.07.003.

952 D’Adamo, S., Schiano di Visconte, G., Lowe, G., Szaub-Newton, J., Beacham, T., Landels, A., Allen, M.
953 J., Spicer, A., and Matthijs, M. (2019). Engineering the unicellular alga *Phaeodactylum*
954 *tricornutum* for high-value plant triterpenoid production. *Plant Biotechnol. J.* 17, 75–87.
955 doi:10.1111/pbi.12948.

956 Dall’Osto, L., Lico, C., Alric, J., Giuliano, G., Havaux, M., and Bassi, R. (2006). Lutein is needed for
957 efficient chlorophyll triplet quenching in the major LHCII antenna complex of higher plants and
958 effective photoprotection in vivo under strong light. *BMC Plant Biol.* 6, 32. doi:10.1186/1471-
959 2229-6-32.

960 Davies, F. K., Jinkerson, R. E., and Posewitz, M. C. (2015). Toward a photosynthetic microbial platform
961 for terpenoid engineering. *Photosyn Res* 123, 265–284. doi:10.1007/s11120-014-9979-6.

962 Della Monica, F., and Kleij, A. W. (2020). From terpenes to sustainable and functional polymers. *Polym.*
963 *Chem.* 11, 5109–5127. doi:10.1039/D0PY00817F.

964 Dellas, N., Thomas, S. T., Manning, G., and Noel, J. P. (2013). Discovery of a metabolic alternative to the
965 classical mevalonate pathway. *Elife* 2, e00672. doi:10.7554/eLife.00672.

966 Domínguez, A., Deive, F. J., Angeles Sanromán, M., and Longo, M. A. (2010). Biodegradation and
967 utilization of waste cooking oil by *Yarrowia lipolytica* CECT 1240. *Eur. J. Lipid Sci. Technol.* 112,
968 1200–1208. doi:10.1002/ejlt.201000049.

969 Drummond, L., Kschowak, M. J., Breitenbach, J., Wolff, H., Shi, Y.-M., Schrader, J., Bode, H. B.,
970 Sandmann, G., and Buchhaupt, M. (2019). Expanding the Isoprenoid Building Block Repertoire

971 with an IPP Methyltransferase from *Streptomyces monomycini*. *ACS Synth. Biol.* 8, 1303–1313.
972 doi:10.1021/acssynbio.8b00525.

973 Ducat, D. C., Avelar-Rivas, J. A., Way, J. C., and Silver, P. A. (2012). Rerouting carbon flux to enhance
974 photosynthetic productivity. *Appl. Environ. Microbiol.* 78, 2660–2668. doi:10.1128/AEM.07901-11.

975 Dugar, D., and Stephanopoulos, G. (2011). Relative potential of biosynthetic pathways for biofuels and
976 bio-based products. *Nat. Biotechnol.* 29, 1074–1078. doi:10.1038/nbt.2055.

977 Dunlop, M. J. (2011). Engineering microbes for tolerance to next-generation biofuels. *Biotechnol Biofuels*
978 4, 32. doi:10.1186/1754-6834-4-32.

979 Dunlop, M. J., Dossani, Z. Y., Szmidt, H. L., Chu, H. C., Lee, T. S., Keasling, J. D., Hadi, M. Z., and
980 Mukhopadhyay, A. (2011). Engineering microbial biofuel tolerance and export using efflux pumps.
981 *Mol. Syst. Biol.* 7, 487. doi:10.1038/msb.2011.21.

982 Eiben, C. B., de Rond, T., Bloszies, C., Gin, J., Chiniqy, J., Baidoo, E. E. K., Petzold, C. J., Hillson, N. J.,
983 Fiehn, O., and Keasling, J. D. (2019). Mevalonate pathway promiscuity enables noncanonical
984 terpene production. *ACS Synth. Biol.* 8, 2238–2247. doi:10.1021/acssynbio.9b00230.

985 Eiben, C. B., Tian, T., Thompson, M. G., Mendez-Perez, D., Kaplan, N., Goyal, G., Chiniqy, J., Hillson,
986 N. J., Lee, T. S., and Keasling, J. D. (2020). Adenosine triphosphate and carbon efficient route to
987 second generation biofuel isopentanol. *ACS Synth. Biol.* 9, 468–474.
988 doi:10.1021/acssynbio.9b00402.

989 Englund, E., Shabestary, K., Hudson, E. P., and Lindberg, P. (2018). Systematic overexpression study to
990 find target enzymes enhancing production of terpenes in *Synechocystis* PCC 6803, using
991 isoprene as a model compound. *Metab. Eng.* 49, 164–177. doi:10.1016/j.ymben.2018.07.004.

992 Fachet, M., Witte, C., Flassig, R. J., Rihko-Struckmann, L. K., McKie-Krisberg, Z., Polle, J. E. W., and
993 Sundmacher, K. (2020). Reconstruction and analysis of a carbon-core metabolic network for
994 *Dunaliella salina*. *BMC Bioinformatics* 21, 1. doi:10.1186/s12859-019-3325-0.

995 Fei, Q., Liang, B., Tao, L., Tan, E. C. D., Gonzalez, R., Henard, C., and Guarnieri, M. (2020). Biological
996 valorization of natural gas for the production of lactic acid: techno-economic analysis and life
997 cycle assessment. *Biochem Eng J*, 107500. doi:10.1016/j.bej.2020.107500.

998 Ferriols, V. M. E. N., Yaginuma, R., Adachi, M., Takada, K., Matsunaga, S., and Okada, S. (2015).
999 Cloning and characterization of farnesyl pyrophosphate synthase from the highly branched
1000 isoprenoid producing diatom *Rhizosolenia setigera*. *Sci. Rep.* 5, 10246. doi:10.1038/srep10246.

1001 Gao, S., Tong, Y., Zhu, L., Ge, M., Zhang, Y., Chen, D., Jiang, Y., and Yang, S. (2017). Iterative
1002 integration of multiple-copy pathway genes in *Yarrowia lipolytica* for heterologous β -carotene
1003 production. *Metab. Eng.* 41, 192–201. doi:10.1016/j.ymben.2017.04.004.

1004 Gao, X., Gao, F., Liu, D., Zhang, H., Nie, X., and Yang, C. (2016). Engineering the methylerythritol
1005 phosphate pathway in cyanobacteria for photosynthetic isoprene production from CO₂. *Energy*
1006 *Environ. Sci.* 9, 1400–1411. doi:10.1039/C5EE03102H.

1007 Gassler, T., Sauer, M., Gasser, B., Egermeier, M., Troyer, C., Causon, T., Hann, S., Mattanovich, D., and
1008 Steiger, M. G. (2020). The industrial yeast *Pichia pastoris* is converted from a heterotroph into an
1009 autotroph capable of growth on CO₂. *Nat. Biotechnol.* 38, 210–216. doi:10.1038/s41587-019-
1010 0363-0.

1011 George, K. W., Thompson, M. G., Kang, A., Baidoo, E., Wang, G., Chan, L. J. G., Adams, P. D., Petzold,
1012 C. J., Keasling, J. D., and Lee, T. S. (2015). Metabolic engineering for the high-yield production of
1013 isoprenoid-based C₅ alcohols in *E. coli*. *Sci. Rep.* 5, 11128. doi:10.1038/srep11128.

1014 George, K. W., Thompson, M. G., Kim, J., Baidoo, E. E. K., Wang, G., Benites, V. T., Petzold, C. J.,
1015 Chan, L. J. G., Yilmaz, S., Turhanen, P., et al. (2018). Integrated analysis of isopentenyl
1016 pyrophosphate (IPP) toxicity in isoprenoid-producing *Escherichia coli*. *Metab. Eng.* 47, 60–72.
1017 doi:10.1016/j.ymben.2018.03.004.

1018 Guo, J., Zhou, Y. J., Hillwig, M. L., Shen, Y., Yang, L., Wang, Y., Zhang, X., Liu, W., Peters, R. J., Chen,
1019 X., et al. (2013). CYP76AH1 catalyzes turnover of miltiradiene in tanshinones biosynthesis and

1020 enables heterologous production of ferruginol in yeasts. *Proc. Natl. Acad. Sci. USA* 110, 12108–
 1021 12113. doi:10.1073/pnas.1218061110.
 1022 Guo, X., Sun, J., Li, D., and Lu, W. (2018). Heterologous biosynthesis of (+)-nootkatone in unconventional
 1023 yeast ' *Yarrowia lipolytica*. *Biochem Eng J* 137, 125–131. doi:10.1016/j.bej.2018.05.023.
 1024 Hartner, F. S., and Glieder, A. (2006). Regulation of methanol utilisation pathway genes in yeasts. *Microb.*
 1025 *Cell Fact.* 5, 39. doi:10.1186/1475-2859-5-39.
 1026 Hausjell, J., Halbwirth, H., and Spadiut, O. (2018). Recombinant production of eukaryotic cytochrome
 1027 P450s in microbial cell factories. *Biosci. Rep.* 38. doi:10.1042/BSR20171290.
 1028 Hayakawa, H., Motoyama, K., Sobue, F., Ito, T., Kawaide, H., Yoshimura, T., and Hemmi, H. (2018).
 1029 Modified mevalonate pathway of the archaeon *Aeropyrum pernix* proceeds via trans-
 1030 anhydromevalonate 5-phosphate. *Proc. Natl. Acad. Sci. USA* 115, 10034–10039.
 1031 doi:10.1073/pnas.1809154115.
 1032 Helfrich, E. J. N., Lin, G.-M., Voigt, C. A., and Clardy, J. (2019). Bacterial terpene biosynthesis:
 1033 challenges and opportunities for pathway engineering. *Beilstein J Org Chem* 15, 2889–2906.
 1034 doi:10.3762/bjoc.15.283.
 1035 Hernandez-Arranz, S., Perez-Gil, J., Marshall-Sabey, D., and Rodriguez-Concepcion, M. (2019).
 1036 Engineering *Pseudomonas putida* for isoprenoid production by manipulating endogenous and
 1037 shunt pathways supplying precursors. *Microb. Cell Fact.* 18, 152. doi:10.1186/s12934-019-1204-
 1038 z.
 1039 Hernandez-Ortega, A., Vinaixa, M., Zebec, Z., Takano, E., and Scrutton, N. S. (2018). A toolbox for
 1040 diverse oxyfunctionalisation of monoterpenes. *Sci. Rep.* 8, 14396. doi:10.1038/s41598-018-
 1041 32816-1.
 1042 Hirokawa, Y., Kubo, T., Soma, Y., Saruta, F., and Hanai, T. (2020). Enhancement of acetyl-CoA flux for
 1043 photosynthetic chemical production by pyruvate dehydrogenase complex overexpression in
 1044 *Synechococcus elongatus* PCC 7942. *Metab. Eng.* 57, 23–30. doi:10.1016/j.ymben.2019.07.012.
 1045 Hu, B., and Lidstrom, M. E. (2014). Metabolic engineering of *Methylobacterium extorquens* AM1 for 1-
 1046 butanol production. *Biotechnol Biofuels* 7, 156. doi:10.1186/s13068-014-0156-0.
 1047 Ignea, C., Pontini, M., Motawia, M. S., Maffei, M. E., Makris, A. M., and Kampranis, S. C. (2018).
 1048 Synthesis of 11-carbon terpenoids in yeast using protein and metabolic engineering. *Nat. Chem.*
 1049 *Biol.* 14, 1090–1098. doi:10.1038/s41589-018-0166-5.
 1050 Jain, S., Caforio, A., and Driessen, A. J. M. (2014). Biosynthesis of archaeal membrane ether lipids.
 1051 *Front. Microbiol.* 5, 641. doi:10.3389/fmicb.2014.00641.
 1052 Johnson, C. W., Salvachúa, D., Rorrer, N. A., Black, B. A., Vardon, D. R., St. John, P. C., Cleveland, N.
 1053 S., Dominick, G., Elmore, J. R., Grundl, N., et al. (2019). Innovative Chemicals and Materials from
 1054 Bacterial Aromatic Catabolic Pathways. *Joule*. doi:10.1016/j.joule.2019.05.011.
 1055 Kang, A., George, K. W., Wang, G., Baidoo, E., Keasling, J. D., and Lee, T. S. (2016). Isopentenyl
 1056 diphosphate (IPP)-bypass mevalonate pathways for isopentenol production. *Metab. Eng.* 34, 25–
 1057 35. doi:10.1016/j.ymben.2015.12.002.
 1058 Kang, A., Meadows, C. W., Canu, N., Keasling, J. D., and Lee, T. S. (2017). High-throughput enzyme
 1059 screening platform for the IPP-bypass mevalonate pathway for isopentenol production. *Metab.*
 1060 *Eng.* 41, 125–134. doi:10.1016/j.ymben.2017.03.010.
 1061 Kang, A., Mendez-Perez, D., Goh, E.-B., Baidoo, E. E. K., Benites, V. T., Beller, H. R., Keasling, J. D.,
 1062 Adams, P. D., Mukhopadhyay, A., and Lee, T. S. (2019). Optimization of the IPP-bypass
 1063 mevalonate pathway and fed-batch fermentation for the production of isoprenol in *Escherichia*
 1064 *coli*. *Metab. Eng.* 56, 85–96. doi:10.1016/j.ymben.2019.09.003.
 1065 Karunanithi, P. S., and Zerbe, P. (2019). Terpene synthases as metabolic gatekeepers in the evolution of
 1066 plant terpenoid chemical diversity. *Front. Plant Sci.* 10, 1166. doi:10.3389/fpls.2019.01166.
 1067 Kim, J., and Park, W. (2014). Oxidative stress response in *Pseudomonas putida*. *Appl. Microbiol.*
 1068 *Biotechnol.* 98, 6933–6946. doi:10.1007/s00253-014-5883-4.

1069 Kim, S. K., Han, G. H., Seong, W., Kim, H., Kim, S.-W., Lee, D.-H., and Lee, S.-G. (2016). CRISPR
1070 interference-guided balancing of a biosynthetic mevalonate pathway increases terpenoid
1071 production. *Metab. Eng.* 38, 228–240. doi:10.1016/j.ymben.2016.08.006.

1072 Kim, S., Lindner, S. N., Aslan, S., Yishai, O., Wenk, S., Schann, K., and Bar-Even, A. (2020). Growth of
1073 *E. coli* on formate and methanol via the reductive glycine pathway. *Nat. Chem. Biol.* 16, 538–545.
1074 doi:10.1038/s41589-020-0473-5.

1075 Kim, S.-J., Yoon, J., Im, D.-K., Kim, Y. H., and Oh, M.-K. (2019). Adaptively evolved *Escherichia coli* for
1076 improved ability of formate utilization as a carbon source in sugar-free conditions. *Biotechnol*
1077 *Biofuels* 12, 207. doi:10.1186/s13068-019-1547-z.

1078 King, J. R., Woolston, B. M., and Stephanopoulos, G. (2017). Designing a New Entry Point into
1079 Isoprenoid Metabolism by Exploiting Fructose-6-Phosphate Aldolase Side Reactivity of
1080 *Escherichia coli*. *ACS Synth. Biol.* 6, 1416–1426. doi:10.1021/acssynbio.7b00072.

1081 Kirby, J., Dietzel, K. L., Wichmann, G., Chan, R., Antipov, E., Moss, N., Baidoo, E. E. K., Jackson, P.,
1082 Gaucher, S. P., Gottlieb, S., et al. (2016). Engineering a functional 1-deoxy-D-xylulose 5-
1083 phosphate (DXP) pathway in *Saccharomyces cerevisiae*. *Metab. Eng.* 38, 494–503.
1084 doi:10.1016/j.ymben.2016.10.017.

1085 Kirby, J., Geiselman, G. M., Yaegashi, J., Kim, J., Zhuang, X., Tran-Gyamfi, M. B., Prael, J.-P.,
1086 Sundstrom, E. R., Gao, Y., Munoz, N., et al. (2021). Further engineering of *R. toruloides* for the
1087 production of terpenes from lignocellulosic biomass. *Biotechnol Biofuels* 14, 101.
1088 doi:10.1186/s13068-021-01950-w.

1089 Kirby, J., and Keasling, J. D. (2009). Biosynthesis of plant isoprenoids: perspectives for microbial
1090 engineering. *Annu. Rev. Plant Biol.* 60, 335–355. doi:10.1146/annurev.arplant.043008.091955.

1091 Kirby, J., Nishimoto, M., Chow, R. W. N., Baidoo, E. E. K., Wang, G., Martin, J., Schackwitz, W., Chan,
1092 R., Fortman, J. L., and Keasling, J. D. (2015). Enhancing Terpene yield from sugars via novel
1093 routes to 1-deoxy-d-xylulose 5-phosphate. *Appl. Environ. Microbiol.* 81, 130–138.
1094 doi:10.1128/AEM.02920-14.

1095 Kuhl, K. P., Cave, E. R., Abram, D. N., and Jaramillo, T. F. (2012). New insights into the electrochemical
1096 reduction of carbon dioxide on metallic copper surfaces. *Energy Environ. Sci.* 5, 7050.
1097 doi:10.1039/c2ee21234j.

1098 Larroude, M., Celinska, E., Back, A., Thomas, S., Nicaud, J.-M., and Ledesma-Amaro, R. (2018). A
1099 synthetic biology approach to transform *Yarrowia lipolytica* into a competitive biotechnological
1100 producer of β -carotene. *Biotechnol. Bioeng.* 115, 464–472. doi:10.1002/bit.26473.

1101 Lauersen, K. J., Baier, T., Wichmann, J., Wördenweber, R., Mussnug, J. H., Hübner, W., Huser, T., and
1102 Kruse, O. (2016). Efficient phototrophic production of a high-value sesquiterpenoid from the
1103 eukaryotic microalga *Chlamydomonas reinhardtii*. *Metab. Eng.* 38, 331–343.
1104 doi:10.1016/j.ymben.2016.07.013.

1105 Lauersen, K. J., Wichmann, J., Baier, T., Kampranis, S. C., Pateraki, I., Møller, B. L., and Kruse, O.
1106 (2018). Phototrophic production of heterologous diterpenoids and a hydroxy-functionalized
1107 derivative from *Chlamydomonas reinhardtii*. *Metab. Eng.* 49, 116–127.
1108 doi:10.1016/j.ymben.2018.07.005.

1109 Lee, H., Baek, J. I., Lee, J.-Y., Jeong, J., Kim, H., Lee, D.-H., Kim, D.-M., and Lee, S.-G. (2021).
1110 Syntrophic co-culture of a methanotroph and heterotroph for the efficient conversion of methane
1111 to mevalonate. *Metab. Eng.* 67, 285–292. doi:10.1016/j.ymben.2021.07.008.

1112 Lee, H. J., Lee, J., Lee, S.-M., Um, Y., Kim, Y., Sim, S. J., Choi, J.-I., and Woo, H. M. (2017). Direct
1113 Conversion of CO₂ to α -Farnesene Using Metabolically Engineered *Synechococcus elongatus*
1114 PCC 7942. *J. Agric. Food Chem.* 65, 10424–10428. doi:10.1021/acs.jafc.7b03625.

1115 Levisson, M., Araya-Cloutier, C., de Bruijn, W. J. C., van der Heide, M., Salvador López, J. M., Daran, J.-
1116 M., Vincken, J.-P., and Beekwilder, J. (2019). Toward developing a yeast cell factory for the

1117 production of prenylated flavonoids. *J. Agric. Food Chem.* 67, 13478–13486.
1118 doi:10.1021/acs.jafc.9b01367.

1119 Li, Q., Fan, F., Gao, X., Yang, C., Bi, C., Tang, J., Liu, T., and Zhang, X. (2017). Balanced activation of
1120 IspG and IspH to eliminate MEP intermediate accumulation and improve isoprenoids production
1121 in *Escherichia coli*. *Metab. Eng.* 44, 13–21. doi:10.1016/j.ymben.2017.08.005.

1122 Li, Z., Jiang, Y., Guengerich, F. P., Ma, L., Li, S., and Zhang, W. (2020). Engineering cytochrome P450
1123 enzyme systems for biomedical and biotechnological applications. *J. Bio. Chem.* 295, 833–849.
1124 doi:10.1016/S0021-9258(17)49939-X.

1125 Liang, W.-F., Cui, L.-Y., Cui, J.-Y., Yu, K.-W., Yang, S., Wang, T.-M., Guan, C.-G., Zhang, C., and Xing,
1126 X.-H. (2017). Biosensor-assisted transcriptional regulator engineering for *Methylobacterium*
1127 *extorquens* AM1 to improve mevalonate synthesis by increasing the acetyl-CoA supply. *Metab.*
1128 *Eng.* 39, 159–168. doi:10.1016/j.ymben.2016.11.010.

1129 Lim, H. G., Eng, T., Banerjee, D., Alarcon, G., Lau, A. K., Park, M.-R., Simmons, B. A., Palsson, B. O.,
1130 Singer, S. W., Mukhopadhyay, A., et al. (2021). Generation of *Pseudomonas putida* KT2440
1131 strains with efficient utilization of xylose and galactose via adaptive laboratory evolution. *ACS*
1132 *Sustain. Chem. Eng.* doi:10.1021/acssuschemeng.1c03765.

1133 Lim, H. G., Fong, B., Alarcon, G., Magurudeniya, H. D., Eng, T., Szubin, R., Olson, C. A., Palsson, B. O.,
1134 Gladden, J. M., Simmons, B. A., et al. (2020). Generation of ionic liquid tolerant *Pseudomonas*
1135 *putida* KT2440 strains via adaptive laboratory evolution. *Green Chem.* 22, 5677–5690.
1136 doi:10.1039/D0GC01663B.

1137 Liu, X., Zhu, X., Wang, H., Liu, T., Cheng, J., and Jiang, H. (2020). Discovery and modification of
1138 cytochrome P450 for plant natural products biosynthesis. *Synthetic and Systems Biotechnology*
1139 5, 187–199. doi:10.1016/j.synbio.2020.06.008.

1140 Liu, Y., Jiang, X., Cui, Z., Wang, Z., Qi, Q., and Hou, J. (2019). Engineering the oleaginous yeast
1141 *Yarrowia lipolytica* for production of α -farnesene. *Biotechnol Biofuels* 12, 296.
1142 doi:10.1186/s13068-019-1636-z.

1143 Liu, Y., Yan, Z., Lu, X., Xiao, D., and Jiang, H. (2016). Improving the catalytic activity of isopentenyl
1144 phosphate kinase through protein coevolution analysis. *Sci. Rep.* 6, 24117.
1145 doi:10.1038/srep24117.

1146 Lund, S., Hall, R., and Williams, G. J. (2019). An Artificial Pathway for Isoprenoid Biosynthesis Decoupled
1147 from Native Hemiterpene Metabolism. *ACS Synth. Biol.* 8, 232–238.
1148 doi:10.1021/acssynbio.8b00383.

1149 Luo, X., Reiter, M. A., d Espaux, L., Wong, J., Denby, C. M., Lechner, A., Zhang, Y., Grzybowski, A. T.,
1150 Harth, S., Lin, W., et al. (2019). Complete biosynthesis of cannabinoids and their unnatural
1151 analogues in yeast. *Nature* 567, 123–126. doi:10.1038/s41586-019-0978-9.

1152 Lyu, Z., Jain, R., Smith, P., Fetchko, T., Yan, Y., and Whitman, W. B. (2016). Engineering the Autotroph
1153 *Methanococcus maripaludis* for Geraniol Production. *ACS Synth. Biol.* 5, 577–581.
1154 doi:10.1021/acssynbio.5b00267.

1155 Martin, V. J. J., Pitera, D. J., Withers, S. T., Newman, J. D., and Keasling, J. D. (2003). Engineering a
1156 mevalonate pathway in *Escherichia coli* for production of terpenoids. *Nat. Biotechnol.* 21, 796–
1157 802. doi:10.1038/nbt833.

1158 Metzger, P., and Largeau, C. (2005). *Botryococcus braunii*: a rich source for hydrocarbons and related
1159 ether lipids. *Appl. Microbiol. Biotechnol.* 66, 486–496. doi:10.1007/s00253-004-1779-z.

1160 Mi, J., Becher, D., Lubuta, P., Dany, S., Tusch, K., Schewe, H., Buchhaupt, M., and Schrader, J. (2014).
1161 De novo production of the monoterpene geranic acid by metabolically engineered
1162 *Pseudomonas putida*. *Microb. Cell Fact.* 13, 170. doi:10.1186/s12934-014-0170-8.

1163 Minty, J. J., Singer, M. E., Scholz, S. A., Bae, C.-H., Ahn, J.-H., Foster, C. E., Liao, J. C., and Lin, X. N.
1164 (2013). Design and characterization of synthetic fungal-bacterial consortia for direct production of

1165 isobutanol from cellulosic biomass. *Proc. Natl. Acad. Sci. USA* 110, 14592–14597.
1166 doi:10.1073/pnas.1218447110.

1167 Mohamed, E. T., Werner, A. Z., Salvachúa, D., Singer, C. A., Szostkiewicz, K., Rafael Jiménez-Díaz, M.,
1168 Eng, T., Radi, M. S., Simmons, B. A., Mukhopadhyay, A., et al. (2020). Adaptive laboratory
1169 evolution of *Pseudomonas putida* KT2440 improves p-coumaric and ferulic acid catabolism and
1170 tolerance. *Metab. Eng. Commun.* 11, e00143. doi:10.1016/j.mec.2020.e00143.

1171 Morales-Sánchez, D., Martínez-Rodríguez, O. A., and Martínez, A. (2017). Heterotrophic cultivation of
1172 microalgae: production of metabolites of commercial interest. *J. Chem. Technol. Biotechnol.* 92,
1173 925–936. doi:10.1002/jctb.5115.

1174 Moser, S., and Pichler, H. (2019). Identifying and engineering the ideal microbial terpenoid production
1175 host. *Appl. Microbiol. Biotechnol.* 103, 5501–5516. doi:10.1007/s00253-019-09892-y.

1176 Moser, S., Strohmeier, G. A., Leitner, E., Plocek, T. J., Vanhessche, K., and Pichler, H. (2018). Whole-cell
1177 (+)-ambrein production in the yeast *Pichia pastoris*. *Metab. Eng. Commun.* 7, e00077.
1178 doi:10.1016/j.mec.2018.e00077.

1179 Nguyen, A. D., Kim, D., and Lee, E. Y. (2020). Unlocking the biosynthesis of sesquiterpenoids from
1180 methane via the methylerythritol phosphate pathway in methanotrophic bacteria, using α -
1181 humulene as a model compound. *Metab. Eng.* 61, 69–78. doi:10.1016/j.ymben.2020.04.011.

1182 Nikel, P. I., and de Lorenzo, V. (2018). *Pseudomonas putida* as a functional chassis for industrial
1183 biocatalysis: From native biochemistry to trans-metabolism. *Metab. Eng.* 50, 142–155.
1184 doi:10.1016/j.ymben.2018.05.005.

1185 Oliver, J. W. K., and Atsumi, S. (2015). A carbon sink pathway increases carbon productivity in
1186 cyanobacteria. *Metab. Eng.* 29, 106–112. doi:10.1016/j.ymben.2015.03.006.

1187 Orita, I., Nishikawa, K., Nakamura, S., and Fukui, T. (2014). Biosynthesis of polyhydroxyalkanoate
1188 copolymers from methanol by *Methylobacterium extorquens* AM1 and the engineered strains
1189 under cobalt-deficient conditions. *Appl. Microbiol. Biotechnol.* 98, 3715–3725.
1190 doi:10.1007/s00253-013-5490-9.

1191 Orsi, E., Beekwilder, J., Peek, S., Eggink, G., Kengen, S. W. M., and Weusthuis, R. A. (2020a). Metabolic
1192 flux ratio analysis by parallel ¹³C labeling of isoprenoid biosynthesis in *Rhodobacter sphaeroides*.
1193 *Metab. Eng.* 57, 228–238. doi:10.1016/j.ymben.2019.12.004.

1194 Orsi, E., Mougiakos, I., Post, W., Beekwilder, J., Dompè, M., Eggink, G., van der Oost, J., Kengen, S. W.
1195 M., and Weusthuis, R. A. (2020b). Growth-uncoupled isoprenoid synthesis in *Rhodobacter*
1196 *sphaeroides*. *Biotechnol Biofuels* 13, 123. doi:10.1186/s13068-020-01765-1.

1197 Orth, J. D., Thiele, I., and Palsson, B. Ø. (2010). What is flux balance analysis? *Nat. Biotechnol.* 28, 245–
1198 248. doi:10.1038/nbt.1614.

1199 Otto, M., Teixeira, P. G., Vizcaino, M. I., David, F., and Siewers, V. (2019). Integration of a multi-step
1200 heterologous pathway in *Saccharomyces cerevisiae* for the production of abscisic acid. *Microb.*
1201 *Cell Fact.* 18, 205. doi:10.1186/s12934-019-1257-z.

1202 Pang, Y., Zhao, Y., Li, S., Zhao, Y., Li, J., Hu, Z., Zhang, C., Xiao, D., and Yu, A. (2019). Engineering the
1203 oleaginous yeast *Yarrowia lipolytica* to produce limonene from waste cooking oil. *Biotechnol*
1204 *Biofuels* 12, 241. doi:10.1186/s13068-019-1580-y.

1205 Park, Y.-K., Nicaud, J.-M., and Ledesma-Amaro, R. (2018). The Engineering Potential of *Rhodospiridium*
1206 *toruloides* as a Workhorse for Biotechnological Applications. *Trends Biotechnol.* 36, 304–317.
1207 doi:10.1016/j.tibtech.2017.10.013.

1208 Pasternak, Z., Pietrokovski, S., Rotem, O., Gophna, U., Lurie-Weinberger, M. N., and Jurkevitch, E.
1209 (2013). By their genes ye shall know them: genomic signatures of predatory bacteria. *ISME J.* 7,
1210 756–769. doi:10.1038/ismej.2012.149.

1211 Pattanaik, B., Englund, E., Nolte, N., and Lindberg, P. (2020). Introduction of a green algal squalene
1212 synthase enhances squalene accumulation in a strain of *Synechocystis* sp. PCC 6803. *Metab.*
1213 *Eng. Commun.* 10, e00125. doi:10.1016/j.mec.2020.e00125.

1214 Pham, J. V., Yilma, M. A., Feliz, A., Majid, M. T., Maffetone, N., Walker, J. R., Kim, E., Cho, H. J.,
1215 Reynolds, J. M., Song, M. C., et al. (2019). A review of the microbial production of bioactive
1216 natural products and biologics. *Front. Microbiol.* 10, 1404. doi:10.3389/fmicb.2019.01404.

1217 Pramastya, H., Xue, D., Abdallah, I. I., Setroikromo, R., and Quax, W. J. (2021). High level production of
1218 amorphadiene using *Bacillus subtilis* as an optimized terpenoid cell factory. *N. Biotechnol.* 60,
1219 159–167. doi:10.1016/j.nbt.2020.10.007.

1220 Primak, Y. A., Du, M., Miller, M. C., Wells, D. H., Nielsen, A. T., Weyler, W., and Beck, Z. Q. (2011).
1221 Characterization of a feedback-resistant mevalonate kinase from the archaeon *Methanosarcina*
1222 *mazei*. *Appl. Environ. Microbiol.* 77, 7772–7778. doi:10.1128/AEM.05761-11.

1223 Rico, J., Duquesne, K., Petit, J.-L., Mariage, A., Darii, E., Peruch, F., de Berardinis, V., and Iacazio, G.
1224 (2019). Exploring natural biodiversity to expand access to microbial terpene synthesis. *Microb.*
1225 *Cell Fact.* 18, 23. doi:10.1186/s12934-019-1074-4.

1226 Ro, D.-K., Paradise, E. M., Ouellet, M., Fisher, K. J., Newman, K. L., Ndungu, J. M., Ho, K. A., Eachus, R.
1227 A., Ham, T. S., Kirby, J., et al. (2006). Production of the antimalarial drug precursor artemisinic
1228 acid in engineered yeast. *Nature* 440, 940–943. doi:10.1038/nature04640.

1229 Rodrigues, J. S., and Lindberg, P. (2021). Metabolic engineering of *Synechocystis* sp. PCC 6803 for
1230 improved bisabolene production. *Metab. Eng. Commun.* 12, e00159.
1231 doi:10.1016/j.mec.2020.e00159.

1232 Sánchez-Pascuala, A., Fernández-Cabezón, L., de Lorenzo, V., and Nikel, P. I. (2019). Functional
1233 implementation of a linear glycolysis for sugar catabolism in *Pseudomonas putida*. *Metab. Eng.*
1234 54, 200–211. doi:10.1016/j.ymben.2019.04.005.

1235 Santos-Merino, M., Torrado, A., Davis, G. A., Röttig, A., Bibby, T. S., Kramer, D. M., and Ducat, D. C.
1236 (2021). Improved photosynthetic capacity and photosystem I oxidation via heterologous
1237 metabolism engineering in cyanobacteria. *Proc. Natl. Acad. Sci. USA* 118.
1238 doi:10.1073/pnas.2021523118.

1239 Schada von Borzyskowski, L., Sonntag, F., Pöschel, L., Vorholt, J. A., Schrader, J., Erb, T. J., and
1240 Buchhaupt, M. (2018). Replacing the Ethylmalonyl-CoA Pathway with the Glyoxylate Shunt
1241 Provides Metabolic Flexibility in the Central Carbon Metabolism of *Methylobacterium extorquens*
1242 AM1. *ACS Synth. Biol.* 7, 86–97. doi:10.1021/acssynbio.7b00229.

1243 Schempp, F. M., Drummond, L., Buchhaupt, M., and Schrader, J. (2018). Microbial cell factories for the
1244 production of terpenoid flavor and fragrance compounds. *J. Agric. Food Chem.* 66, 2247–2258.
1245 doi:10.1021/acs.jafc.7b00473.

1246 Schrader, J., Schilling, M., Holtmann, D., Sell, D., Filho, M. V., Marx, A., and Vorholt, J. A. (2009).
1247 Methanol-based industrial biotechnology: current status and future perspectives of methylotrophic
1248 bacteria. *Trends Biotechnol.* 27, 107–115. doi:10.1016/j.tibtech.2008.10.009.

1249 Sebesta, J., and Peebles, C. A. (2020). Improving heterologous protein expression in *Synechocystis* sp.
1250 PCC 6803 for alpha-bisabolene production. *Metab. Eng. Commun.* 10, e00117.
1251 doi:10.1016/j.mec.2019.e00117.

1252 Soccol, C. R., Dalmas Neto, C. J., Soccol, V. T., Sydney, E. B., da Costa, E. S. F., Medeiros, A. B. P.,
1253 and Vandenberghe, L. P. de S. (2017). Pilot scale biodiesel production from microbial oil of
1254 *Rhodospiridium toruloides* DEBB 5533 using sugarcane juice: Performance in diesel engine and
1255 preliminary economic study. *Bioresour. Technol.* 223, 259–268.
1256 doi:10.1016/j.biortech.2016.10.055.

1257 Song, Y., Guan, Z., van Merkerk, R., Pramastya, H., Abdallah, I. I., Setroikromo, R., and Quax, W. J.
1258 (2020). Production of Squalene in *Bacillus subtilis* by Squalene Synthase Screening and
1259 Metabolic Engineering. *J. Agric. Food Chem.* 68, 4447–4455. doi:10.1021/acs.jafc.0c00375.

1260 Song, Y., He, S., Abdallah, I. I., Jopkiewicz, A., Setroikromo, R., van Merkerk, R., Tepper, P. G., and
1261 Quax, W. J. (2021). Engineering of Multiple Modules to Improve Amorphadiene Production in
1262 *Bacillus subtilis* Using CRISPR-Cas9. *J. Agric. Food Chem.* doi:10.1021/acs.jafc.1c00498.

1263 Sonntag, F., Kroner, C., Lubuta, P., Peyraud, R., Horst, A., Buchhaupt, M., and Schrader, J. (2015).
1264 Engineering *Methylobacterium extorquens* for de novo synthesis of the sesquiterpenoid α -
1265 humulene from methanol. *Metab. Eng.* 32, 82–94. doi:10.1016/j.ymben.2015.09.004.

1266 Sun, J., Zhang, C., Nan, W., Li, D., Ke, D., and Lu, W. (2018). Glycerol improves heterologous
1267 biosynthesis of betulinic acid in engineered *Yarrowia lipolytica*. *Chem Eng Sci* 196, 82–90.
1268 doi:10.1016/j.ces.2018.10.052.

1269 Sun, T., Yu, Y., Wang, K., Ledesma-Amaro, R., and Ji, X.-J. (2021). Engineering *Yarrowia lipolytica* to
1270 produce fuels and chemicals from xylose: A review. *Bioresour. Technol.* 337, 125484.
1271 doi:10.1016/j.biortech.2021.125484.

1272 Sun, W., Xue, H., Liu, H., Lv, B., Yu, Y., Wang, Y., Huang, M., and Li, C. (2020). Controlling Chemo- and
1273 Regioselectivity of a Plant P450 in Yeast Cell toward Rare Licorice Triterpenoid Biosynthesis.
1274 *ACS Catal.* 10, 4253–4260. doi:10.1021/acscatal.0c00128.

1275 Thomas, S. T., Louie, G. V., Lubin, J. W., Lundblad, V., and Noel, J. P. (2019). Substrate Specificity and
1276 Engineering of Mevalonate 5-Phosphate Decarboxylase. *ACS Chem. Biol.* 14, 1767–1779.
1277 doi:10.1021/acscchembio.9b00322.

1278 Tian, T., Kang, J. W., Kang, A., and Lee, T. S. (2019). Redirecting Metabolic Flux via Combinatorial
1279 Multiplex CRISPRi-Mediated Repression for Isopentenol Production in *Escherichia coli*. *ACS*
1280 *Synth. Biol.* 8, 391–402. doi:10.1021/acssynbio.8b00429.

1281 Tsuruta, H., Paddon, C. J., Eng, D., Lenihan, J. R., Horning, T., Anthony, L. C., Regentin, R., Keasling, J.
1282 D., Renninger, N. S., and Newman, J. D. (2009). High-level production of amorpho-4,11-diene, a
1283 precursor of the antimalarial agent artemisinin, in *Escherichia coli*. *PLoS One* 4, e4489.
1284 doi:10.1371/journal.pone.0004489.

1285 Vannice, J. C., Skaff, D. A., Keightley, A., Addo, J. K., Wyckoff, G. J., and Miziorko, H. M. (2014).
1286 Identification in *Haloferax volcanii* of phosphomevalonate decarboxylase and isopentenyl
1287 phosphate kinase as catalysts of the terminal enzyme reactions in an archaeal alternate
1288 mevalonate pathway. *J. Bacteriol.* 196, 1055–1063. doi:10.1128/JB.01230-13.

1289 Vickers, C. E., Williams, T. C., Peng, B., and Cherry, J. (2017). Recent advances in synthetic biology for
1290 engineering isoprenoid production in yeast. *Curr. Opin. Chem. Biol.* 40, 47–56.
1291 doi:10.1016/j.cbpa.2017.05.017.

1292 Volke, D. C., Rohwer, J., Fischer, R., and Jennewein, S. (2019). Investigation of the methylerythritol 4-
1293 phosphate pathway for microbial terpenoid production through metabolic control analysis. *Microb.*
1294 *Cell Fact.* 18, 192. doi:10.1186/s12934-019-1235-5.

1295 von Reuss, S., Domik, D., Lemfack, M. C., Magnus, N., Kai, M., Weise, T., and Piechulla, B. (2018).
1296 Sodorifen Biosynthesis in the Rhizobacterium *Serratia plymuthica* Involves Methylation and
1297 Cyclization of MEP-Derived Farnesyl Pyrophosphate by a SAM-Dependent C-Methyltransferase.
1298 *J. Am. Chem. Soc.* 140, 11855–11862. doi:10.1021/jacs.8b08510.

1299 Vranová, E., Coman, D., and Gruissem, W. (2012). Structure and dynamics of the isoprenoid pathway
1300 network. *Mol. Plant* 5, 318–333. doi:10.1093/mp/sss015.

1301 Wang, P., Wei, W., Ye, W., Li, X., Zhao, W., Yang, C., Li, C., Yan, X., and Zhou, Z. (2019). Synthesizing
1302 ginsenoside Rh2 in *Saccharomyces cerevisiae* cell factory at high-efficiency. *Cell Discov.* 5, 5.
1303 doi:10.1038/s41421-018-0075-5.

1304 Wang, X., Liu, W., Xin, C., Zheng, Y., Cheng, Y., Sun, S., Li, R., Zhu, X.-G., Dai, S. Y., Rentzepis, P. M.,
1305 et al. (2016). Enhanced limonene production in cyanobacteria reveals photosynthesis limitations.
1306 *Proc. Natl. Acad. Sci. USA* 113, 14225–14230. doi:10.1073/pnas.1613340113.

1307 Ward, V. C. A., Chatzivasileiou, A. O., and Stephanopoulos, G. (2018). Metabolic engineering of
1308 *Escherichia coli* for the production of isoprenoids. *FEMS Microbiol. Lett.* 365.
1309 doi:10.1093/femsle/fny079.

1310 Wichmann, J., Baier, T., Wentnagel, E., Lauersen, K. J., and Kruse, O. (2018). Tailored carbon
1311 partitioning for phototrophic production of (E)- α -bisabolene from the green microalga
1312 *Chlamydomonas reinhardtii*. *Metab. Eng.* 45, 211–222. doi:10.1016/j.ymben.2017.12.010.

1313 Wong, J., de Rond, T., d Espaux, L., van der Horst, C., Dev, I., Rios-Solis, L., Kirby, J., Scheller, H., and
1314 Keasling, J. (2018). High-titer production of lathyrane diterpenoids from sugar by engineered
1315 *Saccharomyces cerevisiae*. *Metab. Eng.* 45, 142–148. doi:10.1016/j.ymben.2017.12.007.

1316 Wriessnegger, T., Augustin, P., Engleder, M., Leitner, E., Müller, M., Kaluzna, I., Schürmann, M., Mink,
1317 D., Zellnig, G., Schwab, H., et al. (2014). Production of the sesquiterpenoid (+)-nootkatone by
1318 metabolic engineering of *Pichia pastoris*. *Metab. Eng.* 24, 18–29.
1319 doi:10.1016/j.ymben.2014.04.001.

1320 Wu, W., and Maravelias, C. T. (2018). Synthesis and techno-economic assessment of microbial-based
1321 processes for terpenes production. *Biotechnol Biofuels* 11, 294. doi:10.1186/s13068-018-1285-7.

1322 Xiao, H., Zhang, Y., and Wang, M. (2019). Discovery and engineering of cytochrome p450s for terpenoid
1323 biosynthesis. *Trends Biotechnol.* 37, 618–631. doi:10.1016/j.tibtech.2018.11.008.

1324 Xie, D., Jackson, E. N., and Zhu, Q. (2015). Sustainable source of omega-3 eicosapentaenoic acid from
1325 metabolically engineered *Yarrowia lipolytica*: from fundamental research to commercial
1326 production. *Appl. Microbiol. Biotechnol.* 99, 1599–1610. doi:10.1007/s00253-014-6318-y.

1327 Yadav, V. G., De Mey, M., Lim, C. G., Ajikumar, P. K., and Stephanopoulos, G. (2012). The future of
1328 metabolic engineering and synthetic biology: towards a systematic practice. *Metab. Eng.* 14, 233–
1329 241. doi:10.1016/j.ymben.2012.02.001.

1330 Yaegashi, J., Kirby, J., Ito, M., Sun, J., Dutta, T., Mirsiaghi, M., Sundstrom, E. R., Rodriguez, A., Baidoo,
1331 E., Tanjore, D., et al. (2017). *Rhodospiridium toruloides*: a new platform organism for conversion
1332 of lignocellulose into terpene biofuels and bioproducts. *Biotechnol Biofuels* 10, 241.
1333 doi:10.1186/s13068-017-0927-5.

1334 Yang, C., Gao, X., Jiang, Y., Sun, B., Gao, F., and Yang, S. (2016). Synergy between methylerythritol
1335 phosphate pathway and mevalonate pathway for isoprene production in *Escherichia coli*. *Metab.*
1336 *Eng.* 37, 79–91. doi:10.1016/j.ymben.2016.05.003.

1337 Yang, J., Im, Y., Kim, T. H., Lee, M. J., Cho, S., Na, J.-G., Lee, J., and Oh, B.-K. (2020). Engineering
1338 *Pseudomonas putida* KT2440 to convert 2,3-butanediol to mevalonate. *Enzyme Microb. Technol.*
1339 132, 109437. doi:10.1016/j.enzmictec.2019.109437.

1340 Yang, J., Son, J. H., Kim, H., Cho, S., Na, J.-G., Yeon, Y. J., and Lee, J. (2019). Mevalonate production
1341 from ethanol by direct conversion through acetyl-CoA using recombinant *Pseudomonas putida*, a
1342 novel biocatalyst for terpenoid production. *Microb. Cell Fact.* 18, 168. doi:10.1186/s12934-019-
1343 1213-y.

1344 Yang, X., Jiang, Y., Yang, J., He, J., Sun, J., Chen, F., Zhang, M., and Yang, B. (2015). Prenylated
1345 flavonoids, promising nutraceuticals with impressive biological activities. *Trends Food Sci.*
1346 *Technol.* 44, 93–104. doi:10.1016/j.tifs.2015.03.007.

1347 Yao, F., Liu, S.-C., Wang, D.-N., Liu, Z.-J., Hua, Q., and Wei, L.-J. (2020). Engineering oleaginous yeast
1348 *Yarrowia lipolytica* for enhanced limonene production from xylose and lignocellulosic hydrolysate.
1349 *FEMS Yeast Res* 20. doi:10.1093/femsyr/foaa046.

1350 Ye, R. W., Yao, H., Stead, K., Wang, T., Tao, L., Cheng, Q., Sharpe, P. L., Suh, W., Nagel, E., Arcilla, D.,
1351 et al. (2007). Construction of the astaxanthin biosynthetic pathway in a methanotrophic bacterium
1352 *Methylomonas* sp. strain 16a. *J. Ind. Microbiol. Biotechnol.* 34, 289–299. doi:10.1007/s10295-
1353 006-0197-x.

1354 Ye, R.-P., Ding, J., Gong, W., Argyle, M. D., Zhong, Q., Wang, Y., Russell, C. K., Xu, Z., Russell, A. G.,
1355 Li, Q., et al. (2019). CO₂ hydrogenation to high-value products via heterogeneous catalysis. *Nat.*
1356 *Commun.* 10, 5698. doi:10.1038/s41467-019-13638-9.

1357 Yishai, O., Lindner, S. N., Gonzalez de la Cruz, J., Tenenboim, H., and Bar-Even, A. (2016). The formate
1358 bio-economy. *Curr. Opin. Chem. Biol.* 35, 1–9. doi:10.1016/j.cbpa.2016.07.005.

1359 Yook, S. D., Kim, J., Gong, G., Ko, J. K., Um, Y., Han, S. O., and Lee, S. (2020). High-yield lipid
1360 production from lignocellulosic biomass using engineered xylose-utilizing *Yarrowia lipolytica*.
1361 *Glob. Change Biol. Bioenergy* 12, 670–679. doi:10.1111/gcbb.12699.

1362 Yoshida, R., Yoshimura, T., and Hemmi, H. (2020). Reconstruction of the “Archaeal” Mevalonate Pathway
1363 from the Methanogenic Archaeon *Methanosarcina mazei* in *Escherichia coli* Cells. *Appl. Environ.*
1364 *Microbiol.* 86. doi:10.1128/AEM.02889-19.

1365 Yu, F., Okamoto, S., Harada, H., Yamasaki, K., Misawa, N., and Utsumi, R. (2011). Zingiber zerumbet
1366 CYP71BA1 catalyzes the conversion of α -humulene to 8-hydroxy- α -humulene in zerumbone
1367 biosynthesis. *Cell Mol. Life Sci.* 68, 1033–1040. doi:10.1007/s00018-010-0506-4.

1368 Yuan, L. Z., Rouvière, P. E., Larossa, R. A., and Suh, W. (2006). Chromosomal promoter replacement of
1369 the isoprenoid pathway for enhancing carotenoid production in *E. coli*. *Metab. Eng.* 8, 79–90.
1370 doi:10.1016/j.ymben.2005.08.005.

1371 Zhang, C., Liu, J., Zhao, F., Lu, C., Zhao, G.-R., and Lu, W. (2018). Production of sesquiterpenoid
1372 zerumbone from metabolic engineered *Saccharomyces cerevisiae*. *Metab. Eng.* 49, 28–35.
1373 doi:10.1016/j.ymben.2018.07.010.

1374 Zhang, X., Guan, H., Dai, Z., Guo, J., Shen, Y., Cui, G., Gao, W., and Huang, L. (2015). Functional
1375 Analysis of the Isopentenyl Diphosphate Isomerase of *Salvia miltiorrhiza* via Color
1376 Complementation and RNA Interference. *Molecules* 20, 20206–20218.
1377 doi:10.3390/molecules201119689.

1378 Zhang, X., Wang, D., Duan, Y., Zheng, X., Lin, Y., and Liang, S. (2020). Production of lycopene by
1379 metabolically engineered *Pichia pastoris*. *Biosci. Biotechnol. Biochem.* 84, 463–470.
1380 doi:10.1080/09168451.2019.1693250.

1381 Zheng, Y., Liu, Q., Li, L., Qin, W., Yang, J., Zhang, H., Jiang, X., Cheng, T., Liu, W., Xu, X., et al. (2013).
1382 Metabolic engineering of *Escherichia coli* for high-specificity production of isoprenol and prenol as
1383 next generation of biofuels. *Biotechnol Biofuels* 6, 57. doi:10.1186/1754-6834-6-57.

1384 Zhou, F., and Pichersky, E. (2020). More is better: the diversity of terpene metabolism in plants. *Curr.*
1385 *Opin. Plant Biol.* 55, 1–10. doi:10.1016/j.pbi.2020.01.005.

1386 Zhou, K., Qiao, K., Edgar, S., and Stephanopoulos, G. (2015). Distributing a metabolic pathway among a
1387 microbial consortium enhances production of natural products. *Nat. Biotechnol.* 33, 377–383.
1388 doi:10.1038/nbt.3095.

1389 Zhou, K., Zou, R., Zhang, C., Stephanopoulos, G., and Too, H.-P. (2013). Optimization of amorphadiene
1390 synthesis in *Bacillus subtilis* via transcriptional, translational, and media modulation. *Biotechnol.*
1391 *Bioeng.* 110, 2556–2561. doi:10.1002/bit.24900.

1392 Zu, Y., Prather, K. L., and Stephanopoulos, G. (2020). Metabolic engineering strategies to overcome
1393 precursor limitations in isoprenoid biosynthesis. *Curr. Opin. Biotechnol.* 66, 171–178.
1394 doi:10.1016/j.copbio.2020.07.005.

1395